NATIONAL ADVISORY COMMITTEE FOR AERONAUTICS

TECHNICAL NOTE

No. 1248

WIND-TUNNEL INVESTIGATION OF CONTROL-SURFACE CHARACTERISTICS OF PLAIN AND BALANCED FLAPS WITH SEVERAL TRAILING-EDGE ANGLES ON AN NACA 0009 TAPERED SEMISPAN WING

By H. Page Hoggard, Jr. and Elizabeth G. McKinney

Langley Memorial Aeronautical Laboratory
Langley Field, Va.

Washington
April, 1947

NATIONAL ADVISORY COMMITTEE FOR AERONAUTICS

TECHNICAL NOTE NO. 1248

WIND-TUNNEL INVESTIGATION OF CONTROL-SURFACE CHARACTERISTICS OF PLAIN AND BALANCED FLAPS WITH SEVERAL TRAILING-EDGE ANGLES ON AN NACA 0009 TAPERED SEMISPAN WING

By H. Page Hoggard, Jr. and Elizabeth G. McKinney

SUMMARY

Force tests have been made in the Langley 4- by 6-foot vertical tunnel to determine the aerodynamic characteristics of an NACA 0009 tapered semispan wing equipped with a plain and a balanced flap having three different included angles at the trailing edge.

A comparison was made between lift and hinge-moment parameter values as calculated by existing methods from two-dimensional data and the parameter values measured from the test data obtained. The comparison showed that the differences between the measured values of the lift and hinge-moment parameters and the values calculated from two-dimensional data by lifting-surface theory were, in general, no greater than the differences between the measured values for wings of the same aspect ratio but with different chord distributions.

The effects of overhang, gap, and trailing-edge angle on the lift and hinge-moment parameters were similar to the effects previously found in tests of two-dimensional models. Interference between bevel and overhang was indicated by the fact that the incremental effects of the overhang on the hinge-moment parameters varied as the trailing-edge angle was increased.

INTRODUCTION

A program is being carried out by the NACA for the purpose of correlating section and finite-span data on control surfaces having various overhang and trailing-edge balances. As a part of this program tests have been made previously on a rectangular semispan tail surface (reference 1) and on an elliptical semispan wing (reference 2). Results of these correlations showed that by the application of the Jones' edge-velocity correction (reference 3) to the Prandtl lifting-line theory fair agreement could be obtained between theory and experiment for the slope of the lift curve. Lifting-line-theory calculations of hinge-moment parameters are unsatisfactory in most cases, however, because the chordwise loading induced by streamline curvature, which is neglected by lifting-line theory, may be very important with regard to the hinge-moment parameters. A correction for the effect of streamline curvature on the variation of hinge-moment coefficient with angle of attack was derived (reference 4) for wings of elliptical plan form. Application of this correction to values of the variation of hinge-moment coefficient with angle of attack, computed from lifting-line theory, indicated good agreement with the measured values for the models of references 1 and 2. In reference 5 lifting-surface-theory aspect-ratio corrections were developed for application to both lift and hinge-moment parameters, including the parameter of hinge-moment coefficient against flap deflection. These corrections were applied to the calculated parameters for comparison with the results of the present experimental investigation, which consisted of tests in three-dimensional flow of a tapered semispan wing.

SYMBOLS

The results are given in the form of standard NACA coefficients of forces and moments. The coefficients and symbols used are defined as follows:

C_L lift coefficient (L/qS)

c_l section lift coefficient (l/qc)

C_D drag coefficient (D/qS)

C_m pitching-moment coefficient about 0.40c station at wing center line (M/qSc')

C_h flap hinge-moment coefficient $\left(H/q\bar{c}_f^2 b_f\right)$

c_h flap section hinge-moment coefficient $\left(h/qc_f^2\right)$

where

L twice lift of semispan model

l section lift

D twice drag of semispan model

M twice pitching moment of semispan model

H twice flap hinge moment of semispan model

h flap section hinge moment

q free-stream dynamic pressure $\left(\rho V^2/2\right)$

S twice area of semispan model

c airfoil section chord with flap neutral

c' wing mean aerodynamic chord (M.A.C.)

$$\left(\frac{2}{S}\int_0^{b/2} c^2\,dy\right)$$

$\bar{c}_f$ root-mean-square chord of flap back of hinge line

c_f section chord of flap

b twice span of semispan model

b_f twice span of flap

V air velocity

ρ mass density of air

y lateral distance measured perpendicular to root chord

and

A aspect ratio (b^2/S)

c_b section chord of overhang

α angle of attack of chord line

α_o angle of attack for infinite aspect ratio

δ flap deflection relative to airfoil; positive when trailing edge is deflected downward

ϕ trailing-edge angle - included between upper and lower surfaces of airfoil contour at trailing edge (measured on model)

k constant for determination of jet-boundary corrections for flap hinge moment

E Jones' edge-velocity correction factor (reference 3)

Lift and hinge-moment parameters:

$$c_{L_\alpha} = \left(\frac{\partial C_L}{\partial \alpha}\right)_\delta$$

$$\left(\alpha_\delta\right)_{C_L} = \left(\frac{\partial \alpha}{\partial \delta}\right)_{C_L}$$

$$c_{h_\alpha} = \left(\frac{\partial C_h}{\partial \alpha}\right)_\delta$$

$$c_{h_\delta} = \left(\frac{\partial C_h}{\partial \delta}\right)_\alpha$$

$$\left(c_{m_{C_L}}\right)_\delta = \left(\frac{\partial C_m}{\partial C_L}\right)_\delta$$

$$\left(c_{m_{C_L}}\right)_\alpha = \left(\frac{\partial C_m}{\partial C_L}\right)_\alpha$$

$\left(\frac{\partial c_l}{\partial \alpha_o}\right)_\delta$

$\left(\frac{\partial \alpha_o}{\partial \delta}\right)_{c_l}$

$\left(\frac{\partial c_h}{\partial \alpha_o}\right)_\delta$

$\left(\frac{\partial c_h}{\partial \delta}\right)_{\alpha_o}$

The subscript outside the parentheses indicates the factor held constant in determining the parameter.

APPARATUS, MODEL, AND TESTS

All tests were made in the Langley 4- by 6-foot vertical tunnel, which is described in reference 6.

The tapered semispan wing used in the tests had an NACA 0009 profile (table I) and was built of laminated mahogany to the plan form shown in figure 1. The wing had a tip of revolution. The flap chord was 30 percent of the airfoil chord at each spanwise station. The aspect ratio of the wing and its reflection was 3, and the taper ratio was 0.5.

Three flaps of the same plan form but with different included angles at the trailing edge were used. The plans called for a model having a true-contour flap with a trailing edge angle of 11.6° and two beveled flaps with trailing-edge angles of 20° and 30°. Because of the difficulty of working the thin wooden trailing edge, these angles were not obtained exactly. The flap with airfoil contour had, by measurement of the model, an included angle of 11.1° and the two beveled flaps had angles of 19.8° and 29.6°, respectively, as measured. Each flap was tested with a nose of constant radius and with a 0.35c_f elliptical overhang. (See table II and fig. 1.) The gap

between the nose of the flap and the fixed portion of the wing was 0.005c wide along the entire flap span. Each flap was tested with the gap open and with the gap sealed with impregnated fabric.

The tapered wing was tested as a semispan model by mounting it in the tunnel with the inboard end adjacent to the wall of the tunnel, which thereby acted as a reflection plane (fig. 2). The flow over the model simulated the flow over the right semispan of a complete wing consisting of the test panel and its reflection mounted in an 8- by 6-foot wind tunnel. (See figs. 1 and 2.) The model was supported entirely by the balance frame with a small clearance at the tunnel wall so that all forces and moments acting on the model could be measured. The flap hinge moment was measured by a calibrated torque rod and dial system (reference 2).

The tests were made at a dynamic pressure of 13 pounds per square foot, which corresponds to an air velocity of approximately 72 miles per hour at standard sea-level conditions. The test Reynolds number was 1,400,000 based on the model mean aerodynamic chord of 2.08 feet. The effective Reynolds number (for maximum lift coefficient) was approximately 2,700,000 based on a turbulence factor of 1.93 for this tunnel.

Tunnel-wall corrections, theoretically determined according to the method given in reference 7, were applied to the data. No corrections were made for the effect of gap between the root section and the tunnel wall or the leakage around the supporting torque tube. The corrections applied (by addition) to the tunnel data were as follows:

$$\Delta\alpha = 2.046\ C_{L_T} - 0.266\ C_{L_f} \quad \text{(in deg)}$$

$$\Delta C_L = -0.0152\ C_{L_T}$$

$$\Delta C_D = 0.0303\ C_{L_T}^2$$

$$\Delta C_m = 0.0066\ C_{L_T}$$

$$\Delta C_h = kC_{L_T}$$

where C_{L_T} is the total uncorrected lift coefficient,

C_{L_f} is the uncorrected lift coefficient due to flap deflection, and k is a constant dependent on the chord of the overhang as follows:

c_b/c_f	k
Radius	0.0101
0.35	.0078

DISCUSSION

Lift

A summary of the lift parameters C_{L_α} and $(\alpha_\delta)_{C_L}$ for the various flap configurations, as determined from the lift curves found in figures 3 to 14, is given in table III. The effects of overhang, gap, and trailing-edge angle were, in general, similar to the effects that have been found in tests of two-dimensional models (reference 8). With the gap sealed, an increase in overhang had small and irregular effects on C_{L_α} and usually increased $(\alpha_\delta)_{C_L}$; whereas, with the gap open, an increase in overhang reduced C_{L_α} and usually increased $(\alpha_\delta)_{C_L}$. Both C_{L_α} and $(\alpha_\delta)_{C_L}$ were increased either by sealing the gap or by reducing the trailing-edge angle.

A comparison of the lift-parameter values for the tapered wing of the present investigation with the values for the rectangular and elliptical plan forms of previous investigations (references 1 and 2) showed that the effect of the plan form on C_{L_α} and $(\alpha_\delta)_{C_L}$ is irregular and usually is small (fig. 15).

Hinge Moment

The curves of hinge-moment coefficient plotted against angle of attack are shown in figures 3 to 14. The range of angle of attack over which the flap showed a tendency to oscillate is represented by the dashed portions of the

curves. This oscillation resulted from an alternately stalled and unstalled condition of the flap combined with the action of the elastic torque rod. Similar oscillations may be encountered in flight when a flexible control linkage is used.

The hinge-moment parameters for the various arrangements tested are given in table III. The tangent at $\alpha = 0^\circ$ of the hinge-moment curve for $\delta = 0^\circ$ was used to evaluate C_{h_α}; whereas the difference in hinge-moment coefficient at $\alpha = 0^\circ$ between $\delta = 0^\circ$ and 5° was used to evaluate C_{h_δ}. Although measured at only one point or over a small range, the values of the parameters are useful in comparing the characteristics of the various balances and trailing-edge-angle arrangements tested.

As has been found in tests of two-dimensional models (reference 8), decreasing the balance chord, decreasing the beveled-trailing-edge angle, and, in general, sealing the gap at the flap nose made the values of C_{h_α} and C_{h_δ} become more negative (figs. 3 to 14). The effects of gap, overhang, and trailing-edge angle on C_{h_α} and C_{h_δ} are summarized in figure 16.

The effects of the trailing-edge angle on the increments of the hinge-moment parameters produced by overhang and by gap condition are shown in figure 17. Increases in the trailing-edge angle tended to decrease slightly the effect of the overhang on C_{h_δ} but to increase the effect on C_{h_α}. (See fig. 17(a).) A correlation, presented in reference 9, of data on several different airfoil sections indicated that both the increments ΔC_{h_α} and ΔC_{h_δ} caused by given overhangs were very much smaller when the trailing-edge angle was large than when the trailing-edge angle was small. The data shown in figure 17, however, show an opposite effect on ΔC_{h_α} from that shown in reference 9. A mutual interference appears to exist between the effect of the overhang and the effect of the trailing-edge angle, which interference may account in part for the opposite effect on ΔC_{h_α} shown in figure 17.

The effect of the bevel on the overhang is to decrease the effectiveness of the overhang because the bevel decreases the negative pressure over the portion of the airfoil ahead of the flap hinge (reference 10). The break in the airfoil surface ahead of the overhang, however, creates a disturbance which thickens the boundary layer at the trailing edge and thereby increases the effectiveness of the bevel; the size and location of the disturbance and thus its effect on the boundary-layer thickness depends on the length and shape of the overhang. The relative magnitude of the effects of the mutual interference of bevel and overhang on ΔC_{h_α} and ΔC_{h_δ} will depend on the particular model as well as on the trailing-edge angle. Figure 17(b) shows that increases in the trailing-edge angle increased the increments of C_{h_α} and C_{h_δ} caused by unsealing the gap.

Figure 18 shows a comparison of the effect on flap hinge-moment coefficient of bevel and overhang when found separately and in combination. Except at large flap deflections, the increments of hinge-moment coefficient caused by the addition of the effects of overhang and bevel (each determined separately) were slightly different from the increments caused by overhang and bevel tested in combination. The difference indicates the small interference, previously mentioned, of trailing-edge angle and overhang.

A comparison of the hinge-moment parameter values for the tapered wing of the present investigation with the values for the rectangular and elliptical control surfaces of previous investigations (references 1 and 2) showed that, in general, the plan form has a small and inconsistent effect. (See fig. 15.)

Drag

Although the drag coefficients cannot be considered absolute because of unknown tunnel effects, the relative values may be independent of tunnel effects. The drag-coefficient values as functions of angle of attack at various flap deflections are shown in figures 3 to 14. In figure 19 the drag coefficient is plotted against the lift coefficient with $\alpha = 0^\circ$ and δ varying from 0° to 30° for the plain sealed flap with three different trailing-edge angles. The drag coefficients were approximately the

same for all these arrangements at small lift coefficients and flap deflections. At large flap deflections the lift decreased with an increase of the trailing-edge angle for approximately the same amount of drag.

Pitching Moment

The pitching-moment parameters $\left(C_{m_{C_L}}\right)_\delta$ and $\left(C_{m_{C_L}}\right)_\alpha$ (table III) indicate the position of the aerodynamic center with respect to the 0.40c point of the root chord. When the lift was varied by changing the angle of attack, with the flap neutral, the aerodynamic center was located at 0.28c ± 0.03c for the various flap arrangements tested. The aerodynamic center of lift due to flap deflection was located at 0.58c ± 0.04c. In general, increasing the angle at the trailing edge moved the aerodynamic centers due to angle of attack and to flap deflection forward. (See reference 11.)

Comparison of Calculated Values with Experimental Values of Finite-Wing Characteristics

Table III presents the lift and hinge-moment parameter values as measured from section data for use in calculating finite-span data, as measured from the present experimental data, and as calculated for the finite tapered wing from the section data. The section values for the plain flap were obtained from reference 12; the values for the elliptical-nose-overhang flap with the trailing-edge angle of 11.1° were obtained from reference 8 and were corrected for tunnel effects, before the finite-span parameters were calculated, in a manner similar to the method presented in reference 7. The medium nose referred to in reference 8 had the same nose shape as the elliptical nose tested in the present investigation. Since the section data for the elliptical-nose-overhang flaps with trailing-edge angles of 19.8° and 29.6° were not available, the parameter values were obtained by the addition of the increment caused by the effect of the overhang to the values for the plain flap with beveled trailing edge; any interference between the effects of trailing-edge angle and the effects of overhang have therefore been neglected in estimating the aerodynamic section parameters.

Lifting-line theory was used to calculate the lift and hinge-moment parameters from section data according to the methods suggested in references 4 and 8. The Jones' edge-velocity correction to the lifting-line theory (reference 3) was applied in the computation of C_{L_α} with the substitution of values for E for the elliptical plan form of the same aspect ratio, where E is the ratio of the semiperimeter to the span. The method developed in reference 5 for use on a wing of elliptic plan form was applied in calculating the lift and hinge-moment parameters according to lifting-surface theory.

In most cases, values of the lift parameters (table III) and of the hinge-moment parameters (table III and fig. 20) calculated by lifting-surface theory agreed more closely with the measured values than did values calculated by lifting-line theory with the Jones' edge-velocity correction applied. Differences between the measured values of the lift and hinge-moment parameters and values calculated by lifting-surface theory were, in general, no greater than the differences noted in figure 15 between the measured values for wings of the same aspect ratio but with different chord distributions. For the flap with overhang, lifting-line-theory calculations of the hinge-moment parameters showed almost as good agreement with the measured values as lifting-surface-theory calculations. It appears that lifting-surface theory gives closer agreement between calculated and measured values for C_{h_α} than for C_{h_δ}.

CONCLUSIONS

The results of the present tests in three-dimensional flow of an NACA 0009 tapered semispan wing and a comparison with lift and hinge-moment parameters calculated from two-dimensional-flow data of previous investigations indicated the following conclusions:

1. The effects of overhang, gap, and trailing-edge angle on lift and hinge-moment parameters were, in general, similar to effects which previously had been found in tests of two-dimensional models.

2. Interference between trailing-edge angle and overhang was indicated by the fact that the incremental effects of the overhang on the hinge-moment parameters varied as the trailing-edge angle was increased.

3. Differences between the measured values of the lift and hinge-moment parameters and values calculated from two-dimensional data by lifting-surface theory were, in general, no greater than the difference between the measured values for wings of the same aspect ratio but with different chord distributions.

Langley Memorial Aeronautical Laboratory
National Advisory Committee for Aeronautics
Langley Field, Va., April 2, 1946

REFERENCES

1. Garner, I. Elizabeth: Wind-Tunnel Investigation of Control-Surface Characteristics. XX - Plain and Balanced Flaps on an NACA 0009 Rectangular Semispan Tail Surface. NACA ARR No. L4I11f, 1944.

2. Tamburello, Vito, Smith, Bernard J., and Silvers, H. Norman: Wind-Tunnel Investigation of Control-Surface Characteristics of Plain and Balanced Flaps on an NACA 0009 Elliptical Semispan Wing. NACA ARR No. L5L18, 1946.

3. Jones, Robert T.: Correction of the Lifting-Line Theory for the Effect of the Chord. NACA TN No. 817, 1941.

4. Swanson, Robert S., and Gillis, Clarence L.: Limitations of Lifting-Line Theory for Estimation of Aileron Hinge-Moment Characteristics. NACA CB No. 3L02, 1943.

5. Swanson, Robert S., and Crandall, Stewart M.: Lifting-Surface-Theory Aspect-Ratio Corrections to the Lift and Hinge-Moment Parameters for Full-Span Elevators on Horizontal Tail Surfaces. NACA TN No. 1175, 1947.

6. Ames, Milton B., Jr., and Sears, Richard I.: Pressure-Distribution Investigation of an N.A.C.A. 0009 Airfoil with a 30-Percent-Chord Plain Flap and Three Tabs. NACA TN No. 759, 1940.

7. Swanson, Robert S., and Toll, Thomas A.: Jet-Boundary Corrections for Reflection-Plane Models in Rectangular Wind Tunnels. NACA ARR No. 3E22, 1943.

8. Sears, Richard I.: Wind-Tunnel Data on the Aerodynamic Characteristics of Airplane Control Surfaces. NACA ACR No. 3L08, 1943.

9. Morgan, M. B., and Thomas, H. H. B. M.: Control Surface Design in Theory and Practice. Jour. R.A.S., vol. XLIX, no. 416, Aug. 1945, pp. 431-514.

10. Hoggard, H. Page, Jr., and Bulloch, Marjorie E.: Wind-Tunnel Investigation of Control-Surface Characteristics. XVI - Pressure Distribution over an NACA 0009 Airfoil with 0.30-Airfoil-Chord Beveled-Trailing-Edge Flaps. NACA ARR No. L4D03, 1944.

11. Purser, Paul E., and Johnson, Herold S.: Effects of Trailing-Edge Modifications on Pitching-Moment Characteristics of Airfoils. NACA CB No. L4I30, 1944.

12. Langley Research Department: Summary of Lateral-Control Research. (Compiled by Thomas A. Toll.) NACA TN No. 1245, 1947.

TABLE I

ORDINATES FOR NACA 0009 Airfoil

[All dimensions in percent chord]

Station	Ordinates	
	Upper	Lower
0	0	0
1.25	1.42	-1.42
2.5	1.96	-1.96
5.0	2.67	-2.67
7.5	3.15	-3.15
10	3.51	-3.51
15	4.01	-4.01
20	4.30	-4.30
25	4.46	-4.46
30	4.50	-4.50
40	4.35	-4.35
50	3.97	-3.97
60	3.42	-3.42
70	2.75	-2.75
80	1.97	-1.97
90	1.09	-1.09
95	.61	-.61
100	(.10)	(-.10)
100	0	0
L. E. radius, 0.89		

TABLE II

ELLIPTICAL-OVERHANG PROFILE

[All dimensions in percent chord]

Root section		Tip section	
Station	Ordinate	Station	Ordinate
0	0	0	0
.31	.75	.61	1.04
.62	1.05	1.22	1.45
.93	1.28	1.83	1.73
1.25	1.46	2.44	1.97
1.87	1.75	3.66	2.30
2.49	1.98	4.88	2.54
3.11	2.17	6.10	2.69
4.67	2.50	9.16	2.81
6.23	2.70	10.50	2.75
9.34	2.80		
10.50	2.75		
L.E. radius, 1.12		L.E. radius, 1.22	

TABLE III

PARAMETER VALUES FOR A 0.30c FLAP ON A TAPERED SEMISPAN WING

Model characteristics				Section characteristics				Finite-span characteristics												
								$\left(\frac{\partial c_L}{\partial \alpha}\right)_\delta$			$\left(\frac{\partial \alpha}{\partial \delta}\right)_{c_L}$		$\left(\frac{\partial c_h}{\partial \alpha}\right)_\delta$			$\left(\frac{\partial c_h}{\partial \delta}\right)_\alpha$			$\left(\frac{\partial c_m}{\partial c_L}\right)_\delta$	$\left(\frac{\partial c_m}{\partial c_L}\right)_\alpha$
ϕ (deg)	$\frac{c_b}{c_f}$	Gap	Balance nose shape	$\left(\frac{\partial c_l}{\partial \alpha_o}\right)_\delta$	$\left(\frac{\partial \alpha_o}{\partial \delta}\right)_{c_l}$	$\left(\frac{\partial c_h}{\partial \alpha_o}\right)_\delta$	$\left(\frac{\partial c_h}{\partial \delta}\right)_{\alpha_o}$	Measured value	Lifting line theory (a)	Lifting surface theory (b)	Measured value	Lifting surface theory (b)	Measured value	Lifting line theory (a)	Lifting surface theory (b)	Measured value	Lifting line theory (a)	Lifting surface theory (b)	Measured value	Measured value
11.1	-	Sealed	Plain	0.100	-0.59	-0.0058	-0.0119	0.054	0.057	0.053	-0.65	-0.62	-0.0021	-0.0034	-0.0020	-0.0092	-0.0100	-0.0092	0.102	-0.166
11.1	—	0.005c	Plain	.096	.60	-.0063	-.0117	.053	.055	.052	-.57	-.63	-.0030	-.0037	.0023	- 0089	-.0098	.0091	.089	-.180
11 1	0.35	Sealed	Elliptical	.096	.60	-.0030	-.0073	.053	.055	.052	-.65	-.63	-.0015	-.0017	-.0007	-.0060	-.0064	-.0055	.090	-.153
11 1	.35	0.005c	Elliptical	.090	- .55	-.0029	-.0062	.052	.053	.050	-.55	-.58	-.0013	-.0017	-.0007	-.0053	-.0053	-.0046	.096	-.221
19.8	—	Sealed	Plain	.095	- .57	-.0022	-.0085	.053	.055	.052	-.58	-.60	-.0002	-.0013	-.0001	-.0065	-.0079	-.0068	.109	-.158
19.8	—	0.005c	Plain	.090	- .54	-.0019	-.0066	.051	.053	.050	-.53	-.57	-.0003	-.0011	0	-.0053	-.0060	-.0052	.116	-.181
19.8	35	Sealed	Elliptical	.091	- 58	.0006	-.0039	.052	.053	.050	-.63	-.61	.0004	.0003	.0013	-.0040	-.0042	-.0031	110	-.170
19.8	35	0.005c	Elliptical	.084	- .49	.0015	-.0011	.050	.050	.047	-.54	-.51	.0016	.0010	.0019	-.0026	-.0014	-.0005	.132	-.185
29.6	—	Sealed	Plain	.091	-.55	.0018	-.0046	.050	.053	.050	- .50	-.58	.0024	.0011	.0020	-.0016	-.0052	-.0042	.124	-.168
29.6	—	0.005c	Plain	.086	-.46	.0031	-.0008	.048	.051	.048	-.46	-.48	.0034	.0018	.0026	-.0001	-.0014	-.0007	.133	- 139
29.6	.35	Sealed	Elliptical	.087	-.56	.0046	0	.051	.052	.049	-.53	-.59	.0042	.0029	.0036	-.0001	-.0013	-.0003	.135	-.154
29.6	35	0.005c	Elliptical	.080	-.41	.0065	.0047	.047	.049	.046	-.48	-.43	.0062	.0041	.0048	.0020	.0032	.0042	.136	-.179

[a]Calculated with edge-velocity correction (reference 3)

[b]Calculated by method in reference 5.

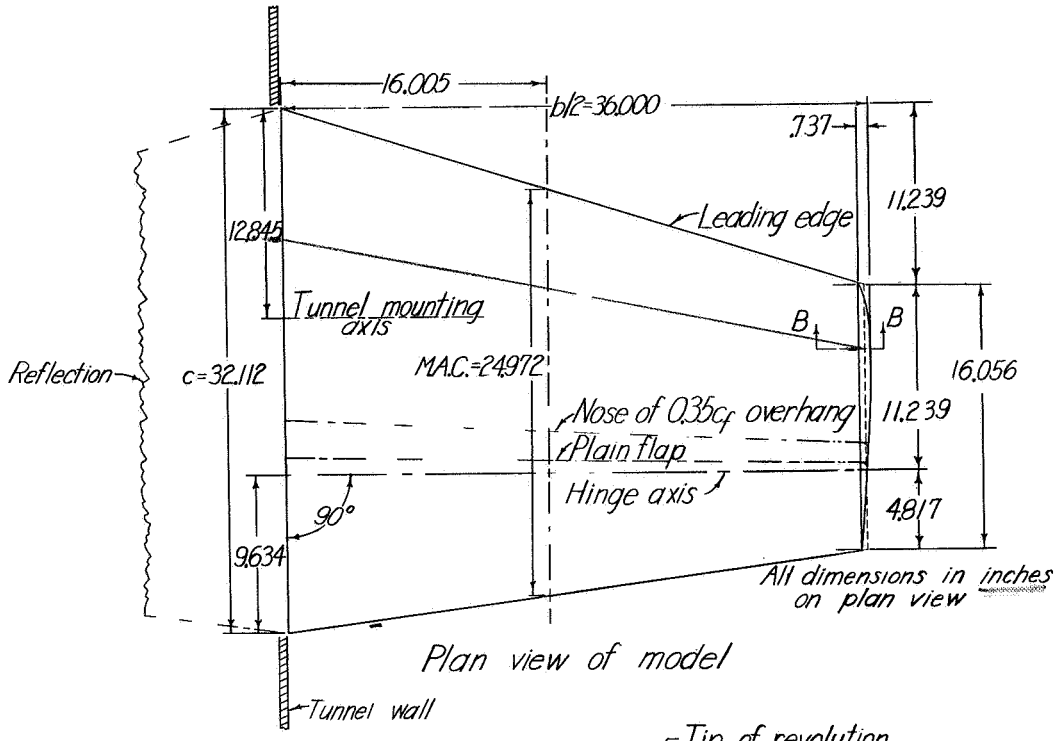

Plan view of model

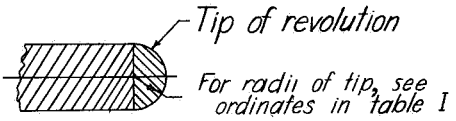

Section B-B

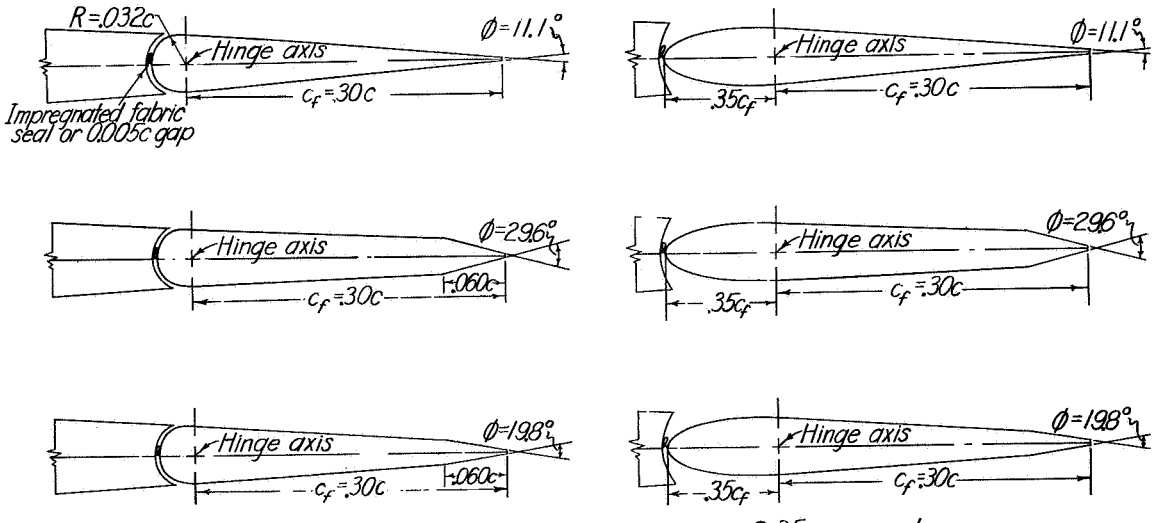

Plain flap

0.35c_f overhang

All of the overhang, gap, and beveled-trailing-edge combinations tested are shown by the above views.

NATIONAL ADVISORY COMMITTEE FOR AERONAUTICS

Figure 1 Details of an NACA 0009 tapered semispan wing. Aspect ratio, 3; area of model and its reflection, 12 square feet, taper ratio, 0.5, $c_f/c = 0.3$. See table II for ordinates of elliptical nose.

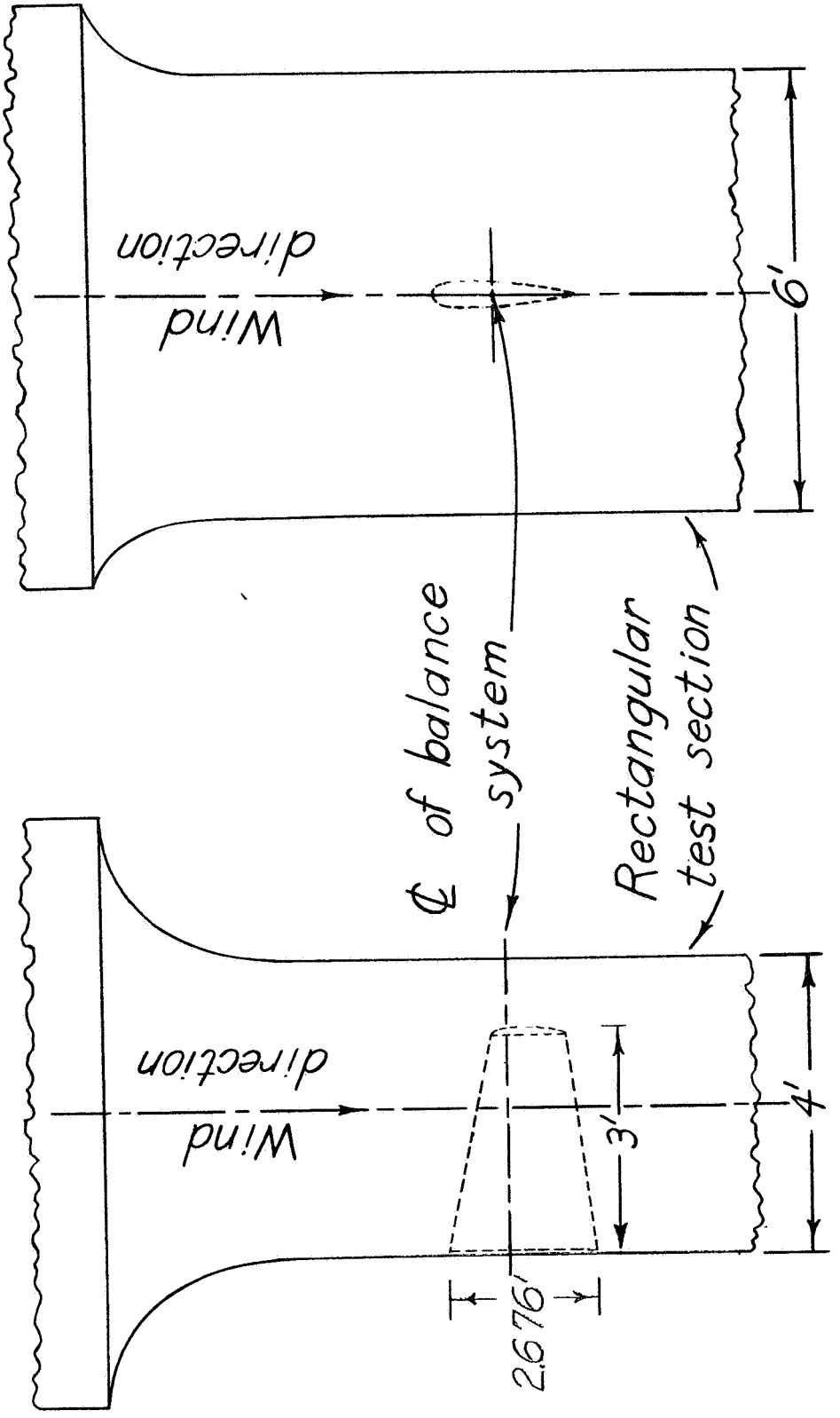

NATIONAL ADVISORY COMMITTEE FOR AERONAUTICS

Figure 2.-Semispan model mounted in the Langley 4-by 6-foot vertical tunnel.

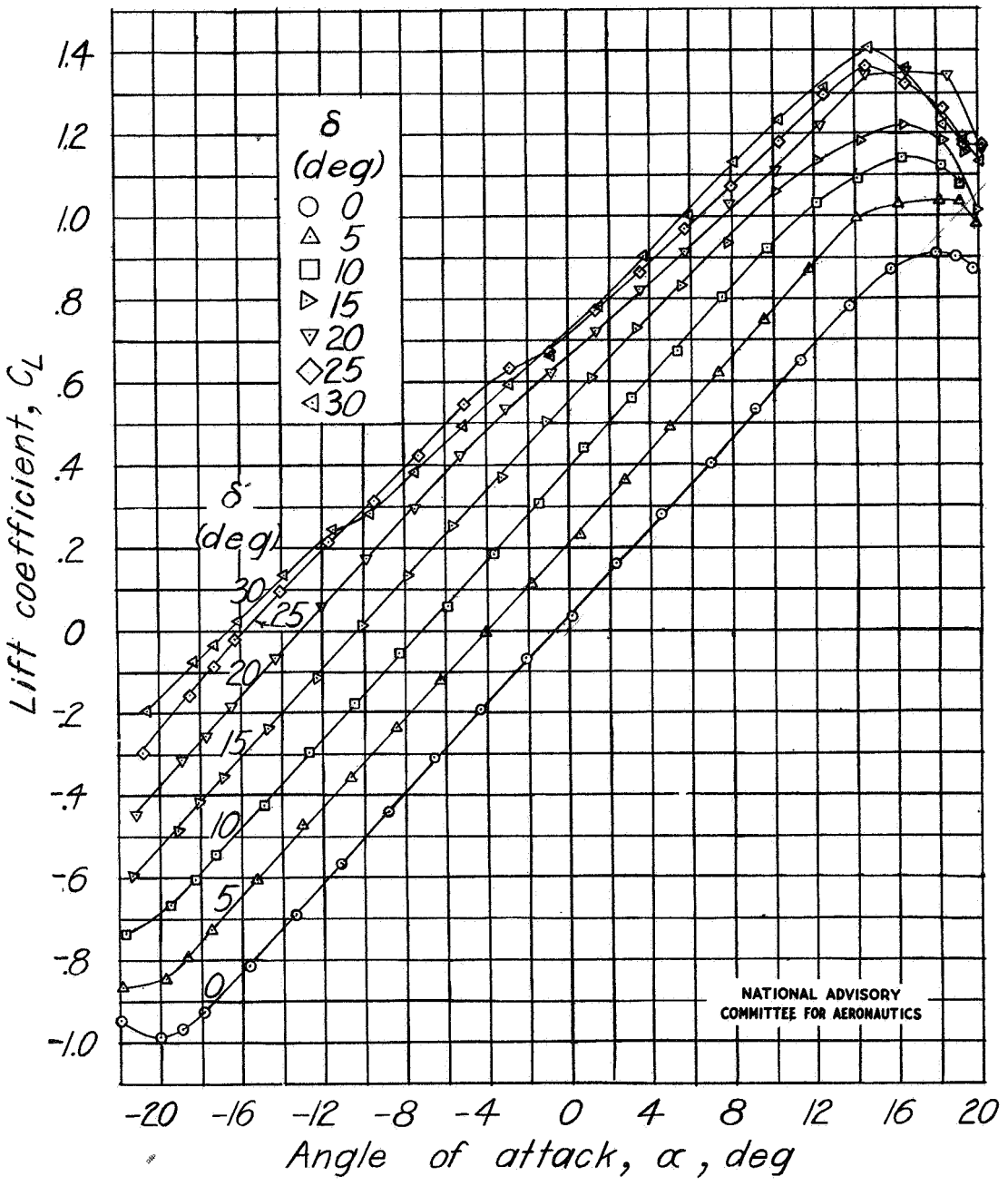

Figure 3.-Aerodynamic characteristics of a tapered semispan wing having a 0.30c plain flap. Sealed gap; $\phi = 11.1^\circ$; $A = 3$.

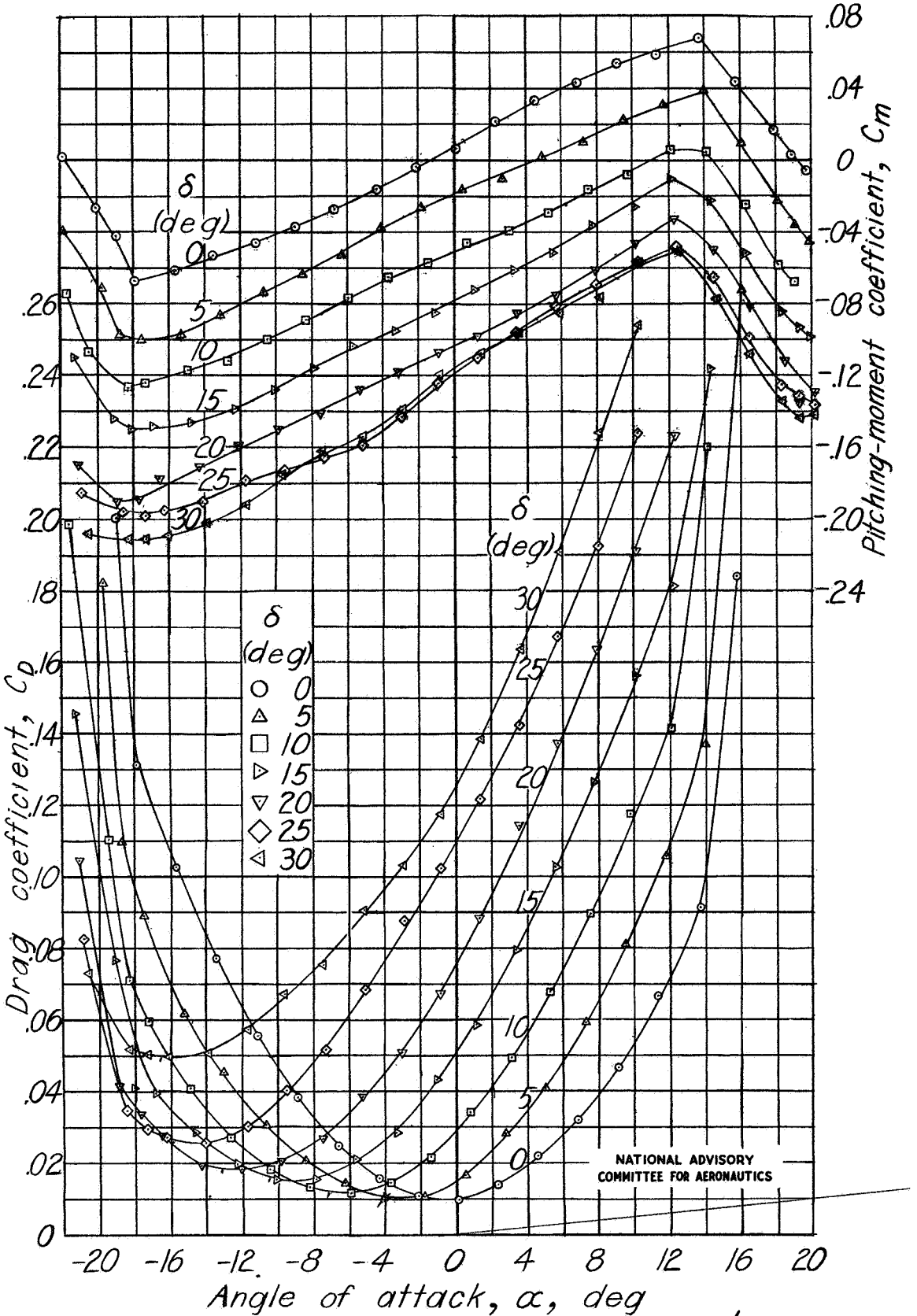

Figure 3 .-Continued. Plain flap; sealed gap; $\phi = 11.1°$.

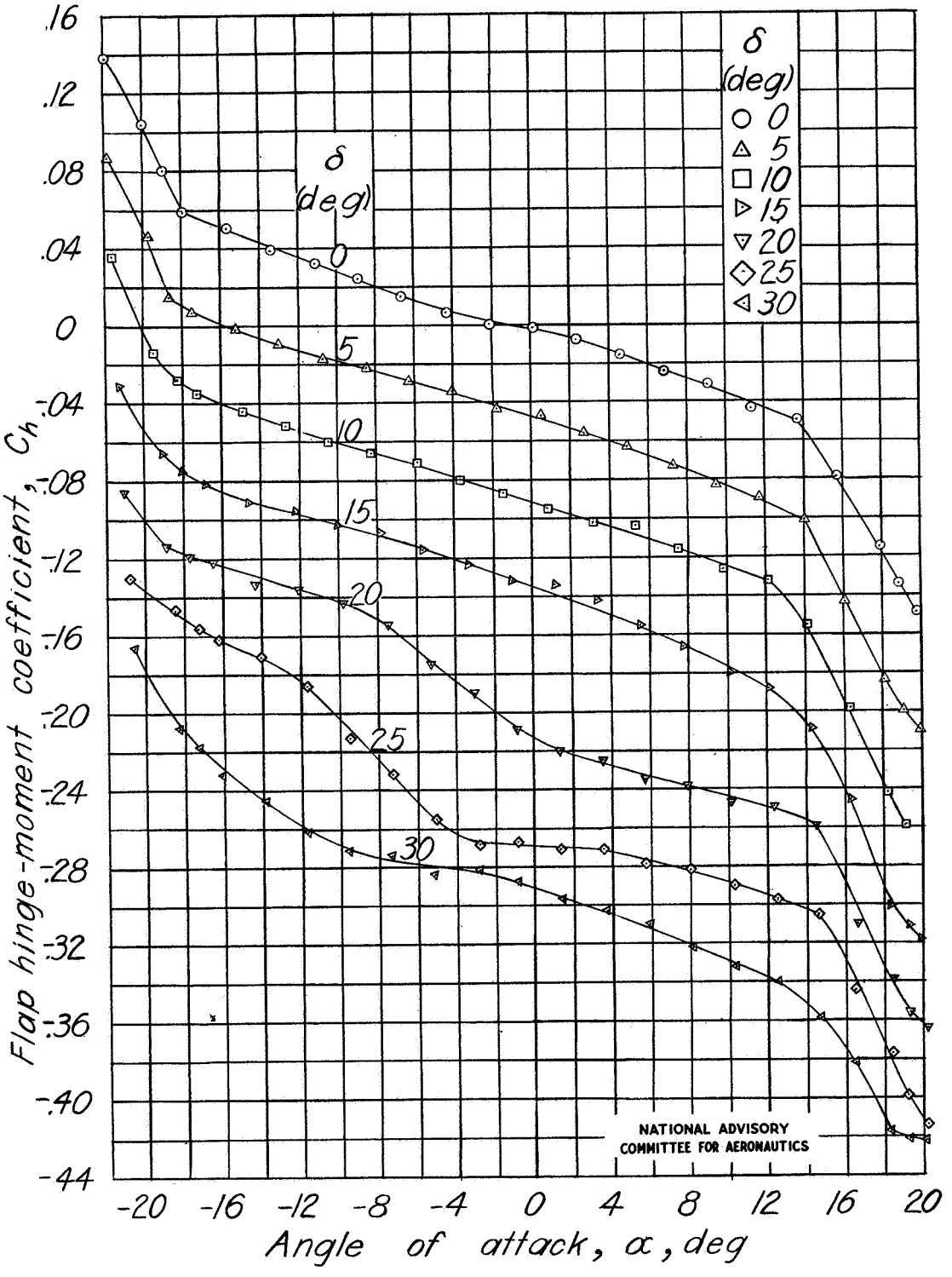

Figure 3.-Concluded. Plain flap; sealed gap; $\phi = 11.1°$.

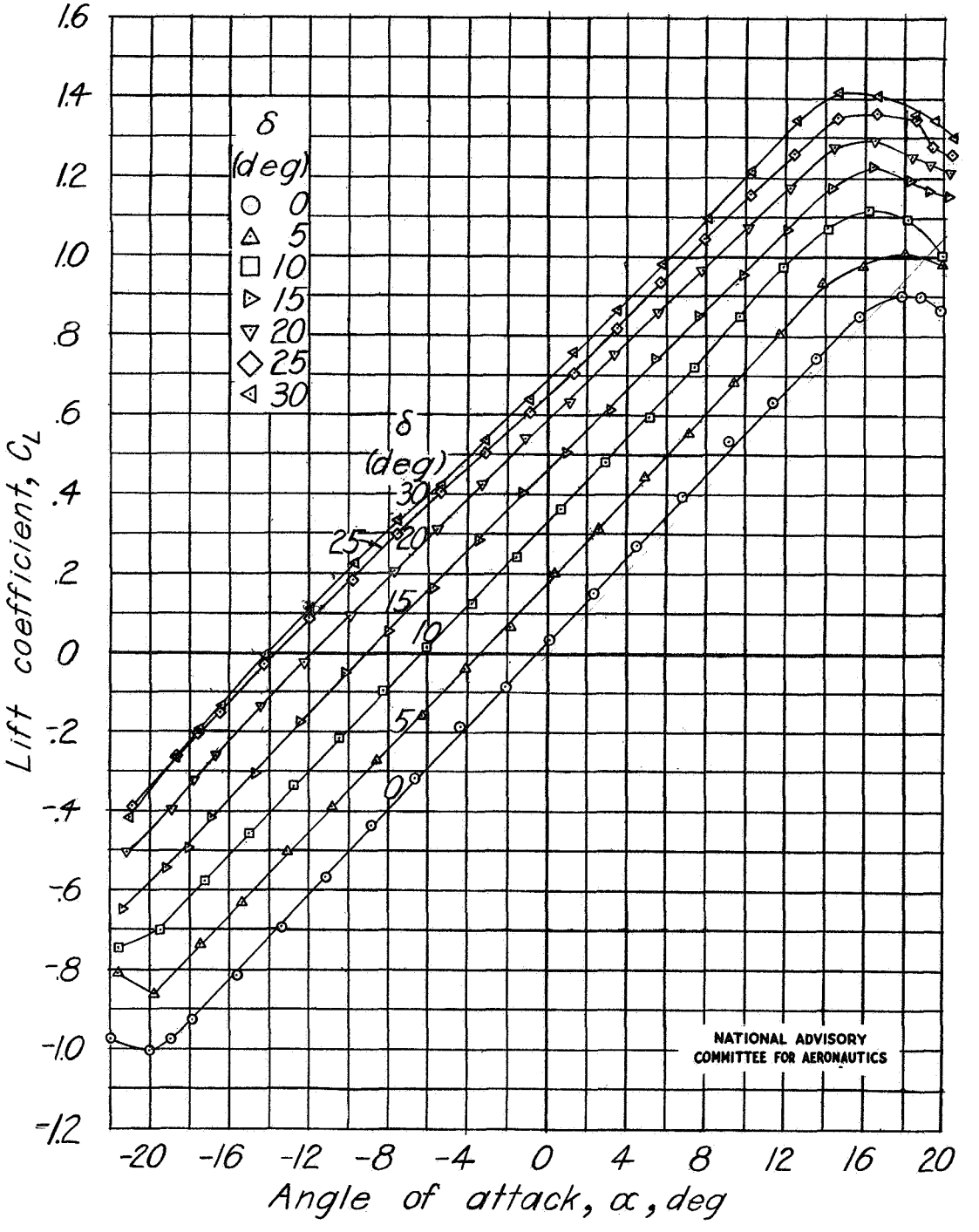

Figure 4.- Aerodynamic characteristics of a tapered semispan wing having a 0.30c plain flap. 0.005c gap; $\phi = 11.1°$; $A = 3$.

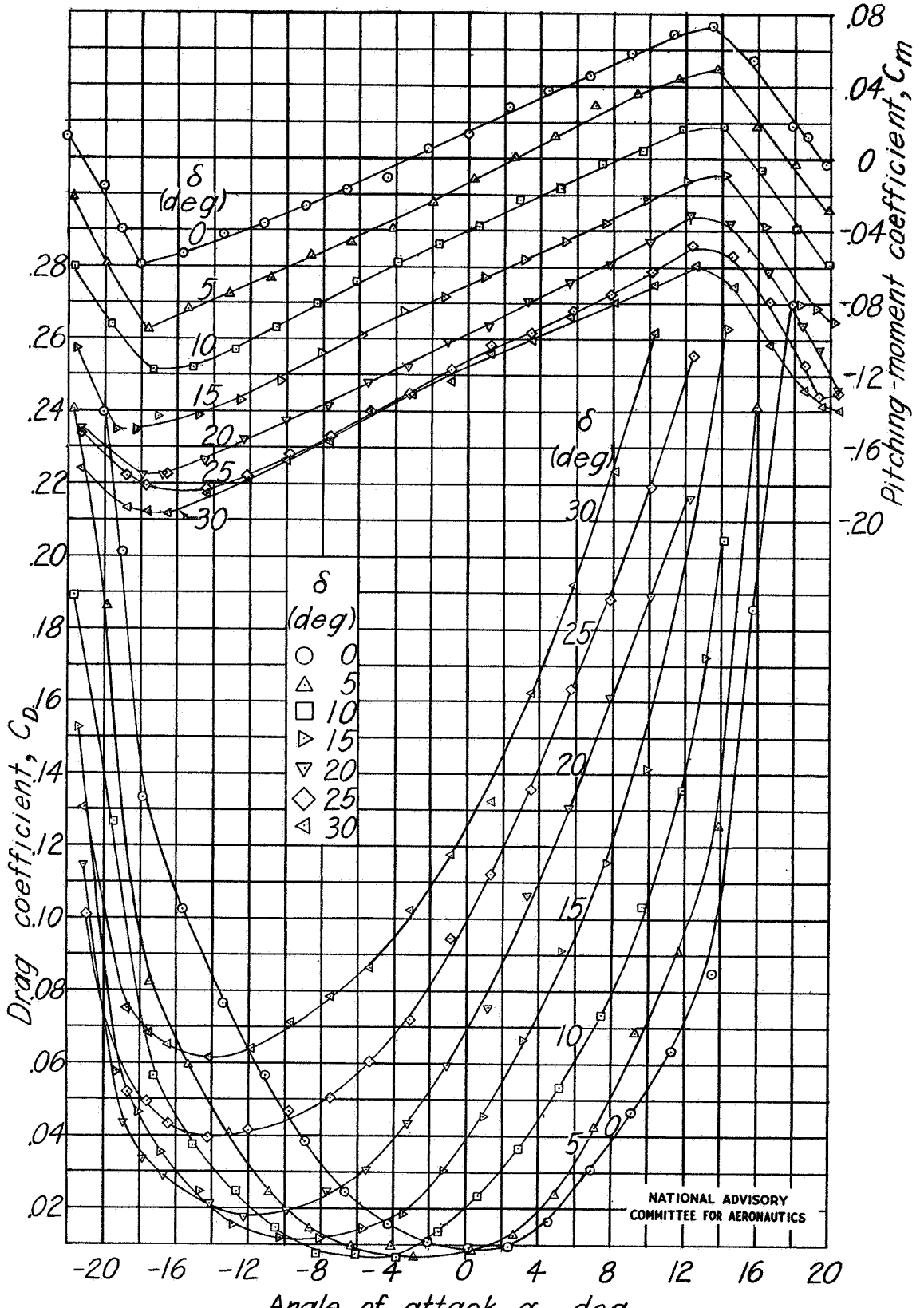

Figure 4 .- Continued. Plain flap; 0.005c gap; $\phi = 11.1°$.

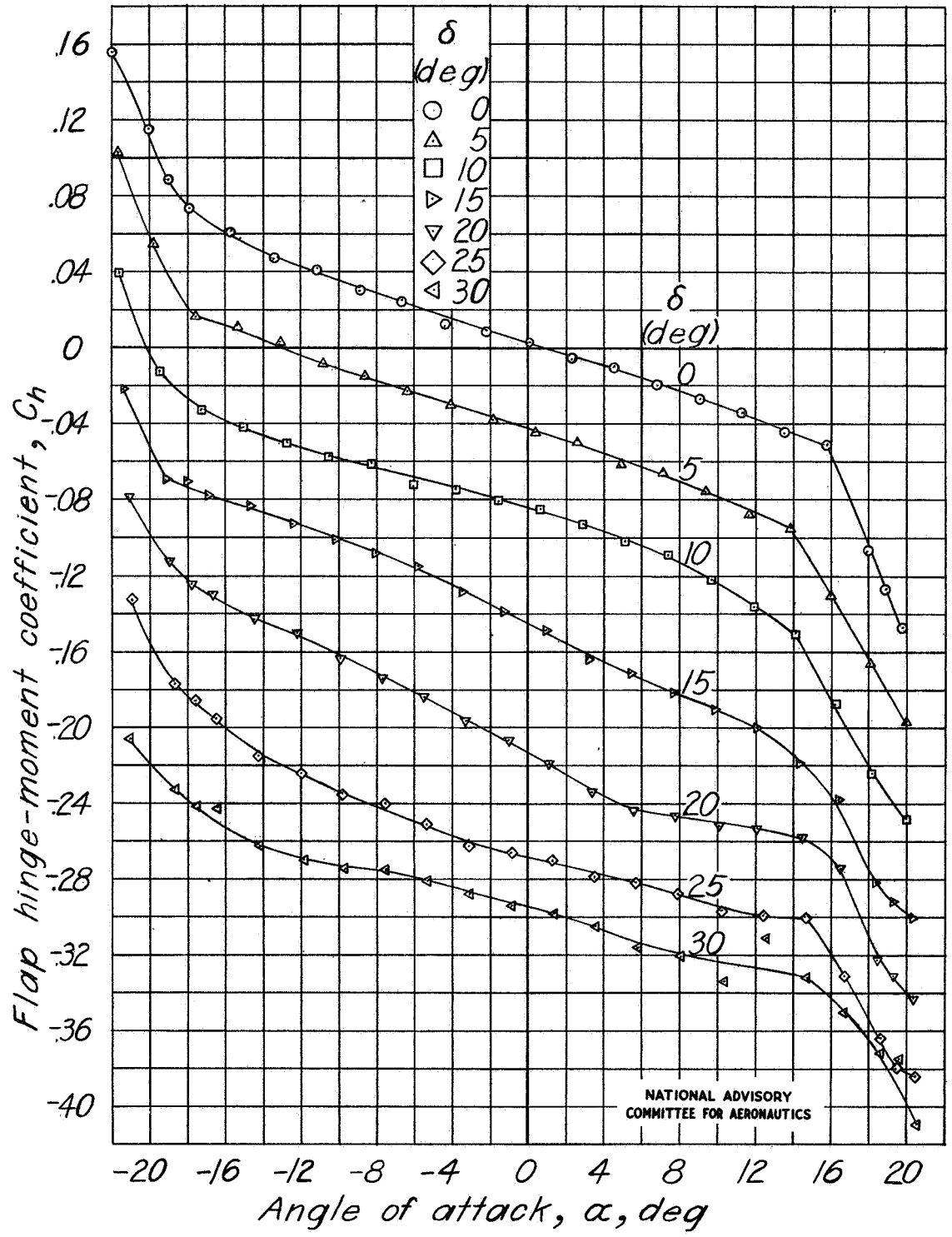

Figure 4.- Concluded. Plain flap; 0.005c gap; ϕ=11.1°

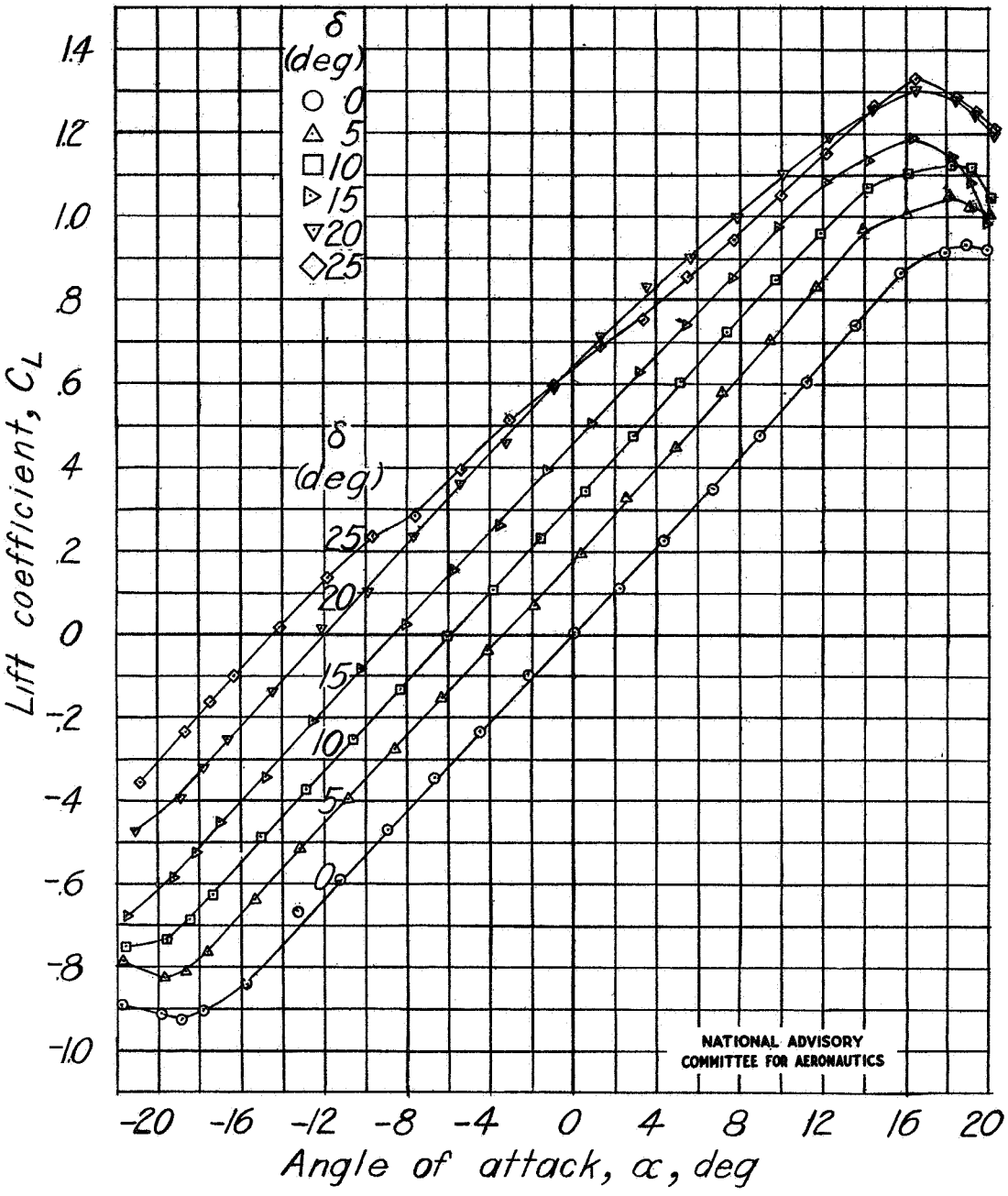

Figure 5 .- Aerodynamic characteristics of a tapered semispan wing having a 0.30c flap with $0.35c_f$ elliptical overhang. Sealed gap; $\Phi = 11.1°$; $A = 3$.

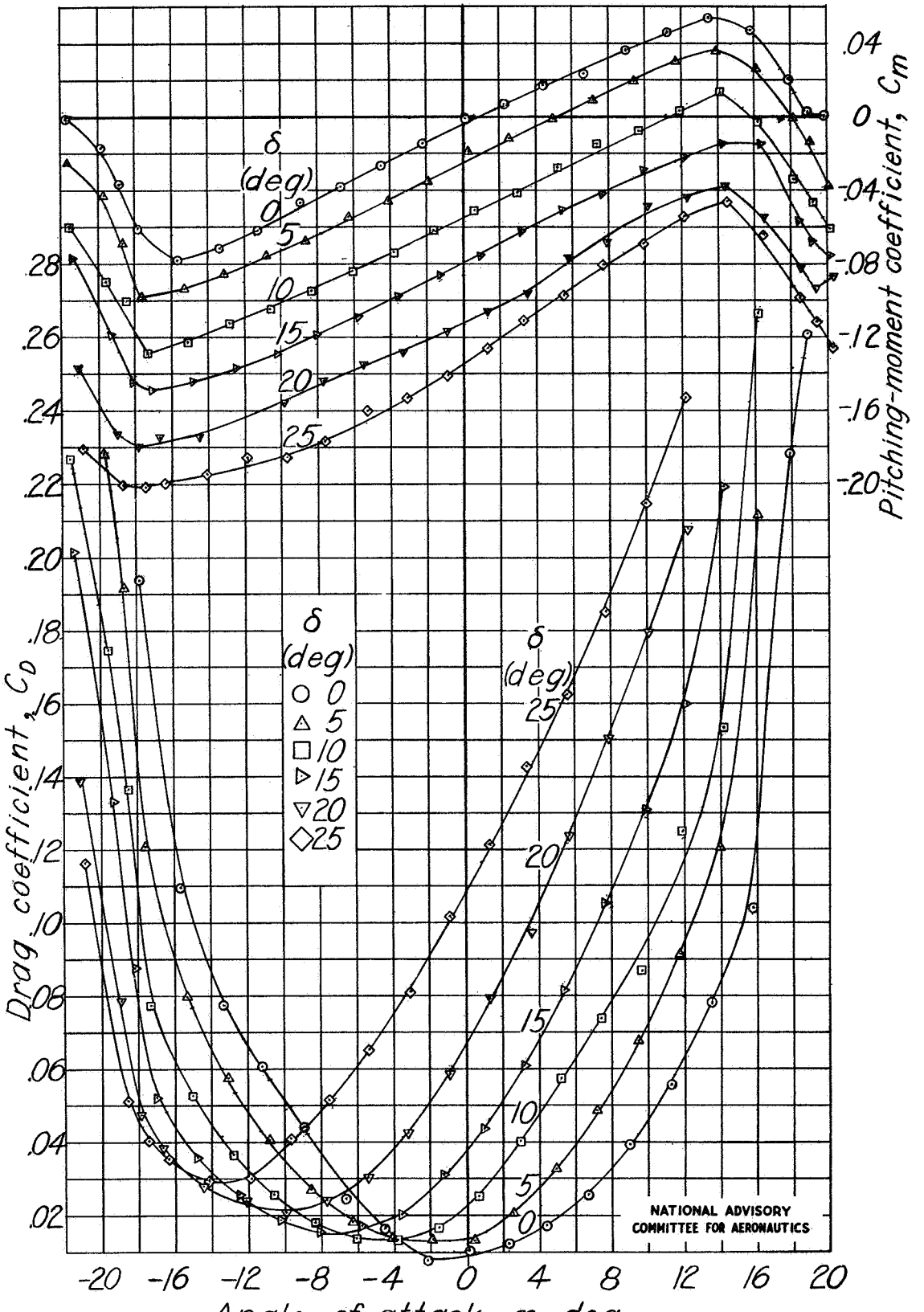

Figure 5 .- Continued. 0.35c_f overhang; sealed gap; $\emptyset$=11.1°.

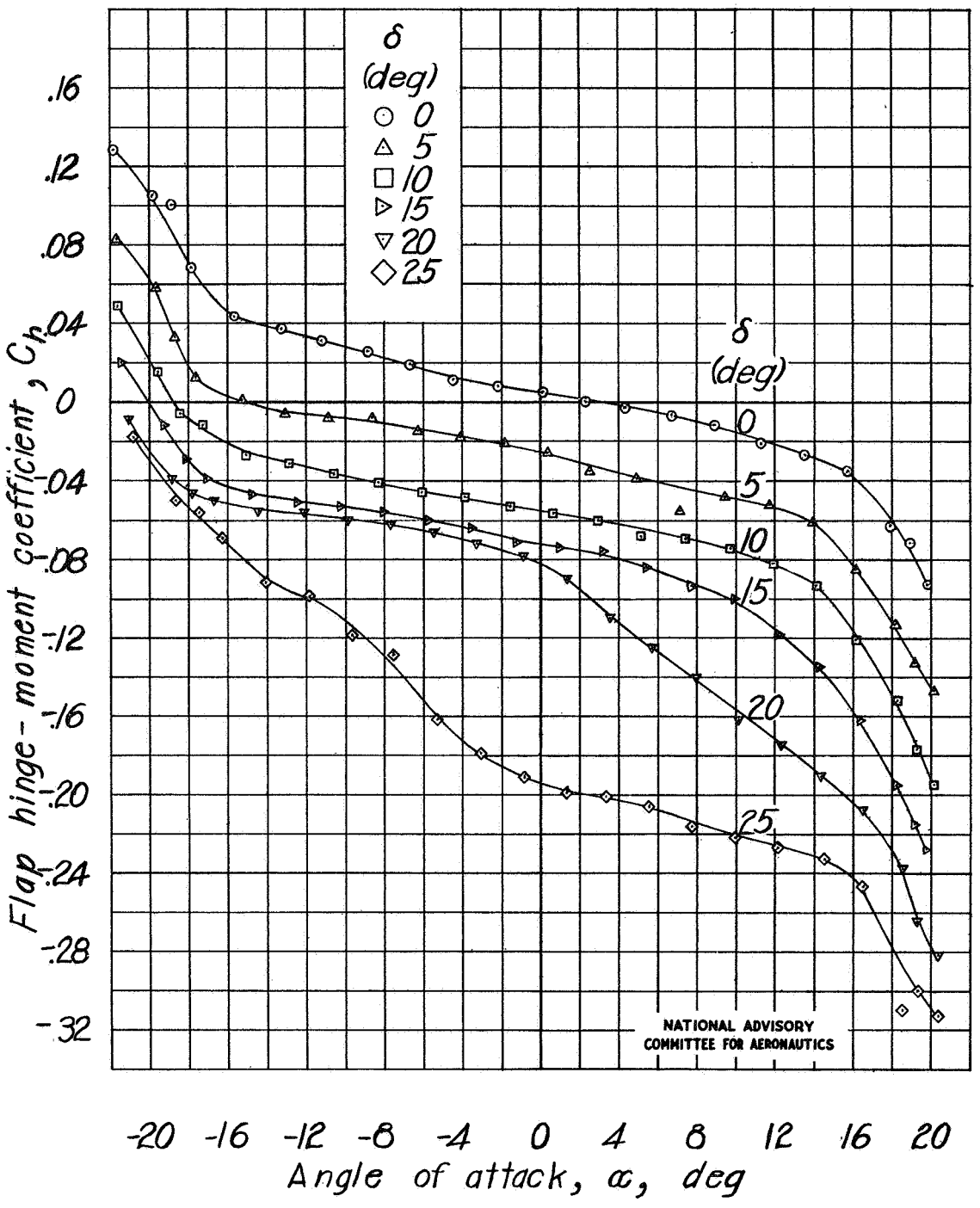

Figure 5.- Concluded. 0.35c_f overhang; sealed gap; $\emptyset$=11.1°.

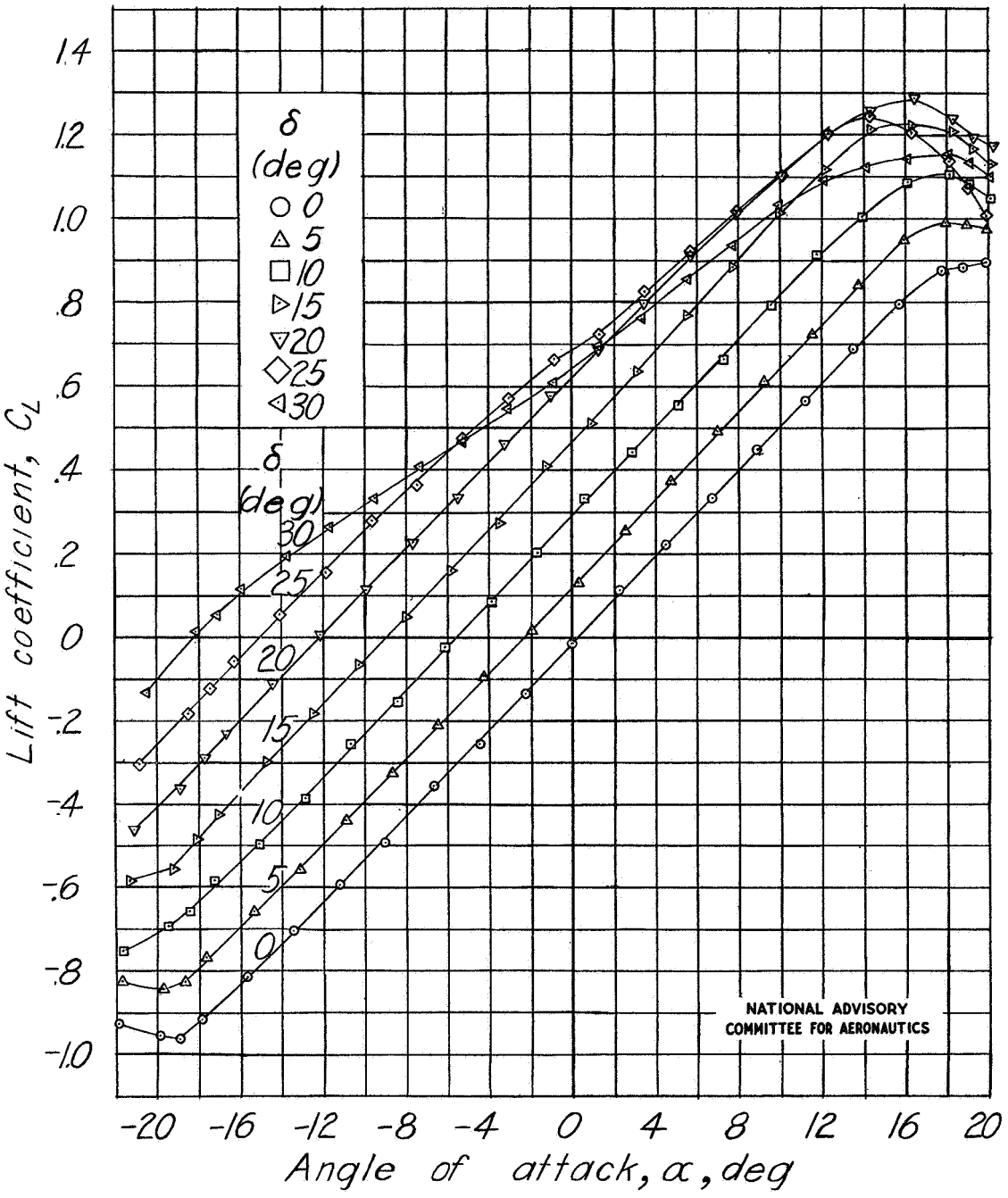

Figure 6 .- Aerodynamic characteristics of a tapered semispan wing having a 0.30c flap with 0.35c_f elliptical overhang. 0.005c gap; $\Phi = 11.1°$; A=3.

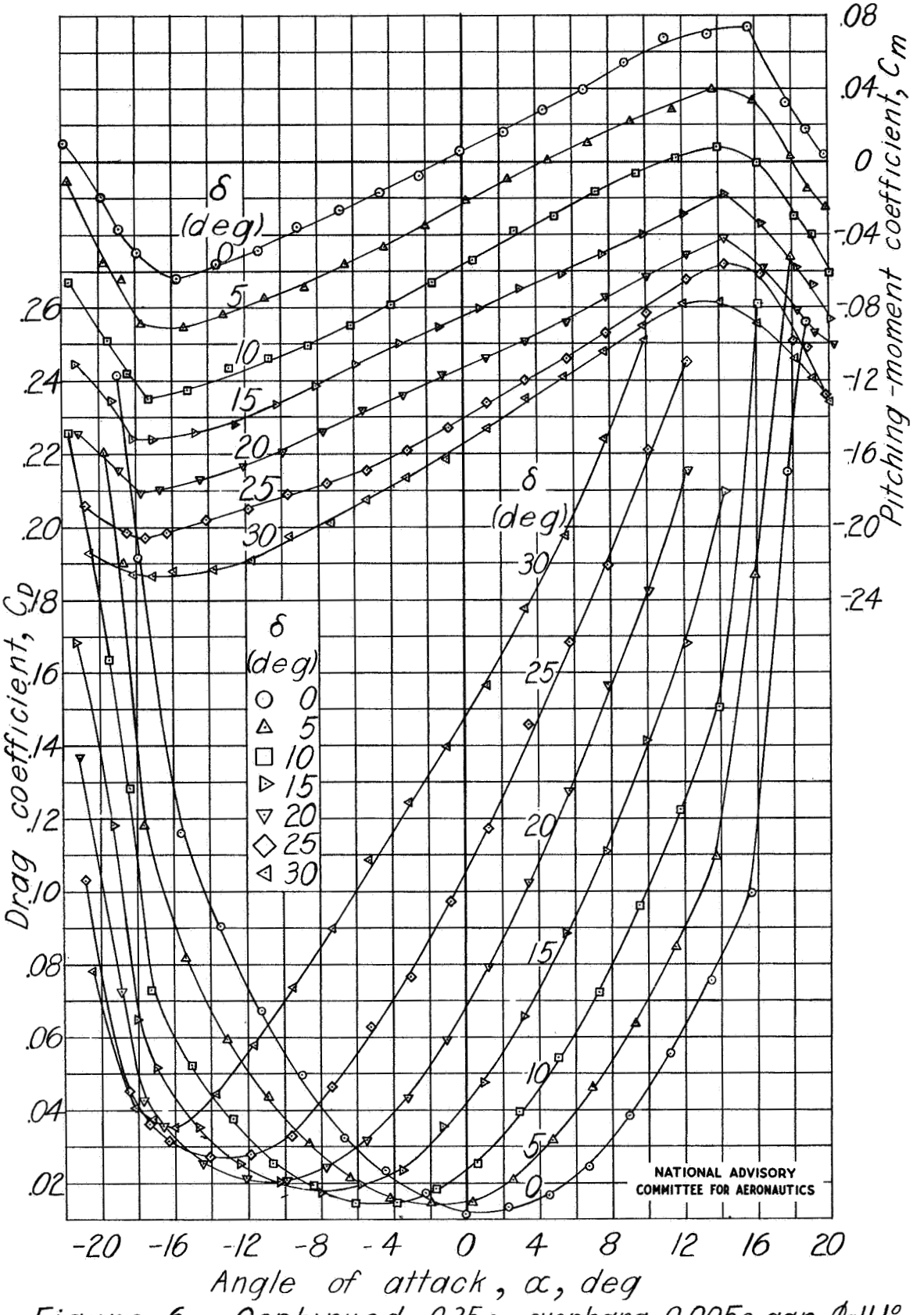

Figure 6.- Continued. 0.35c_f overhang; 0.005c gap; ϕ=11.1°.

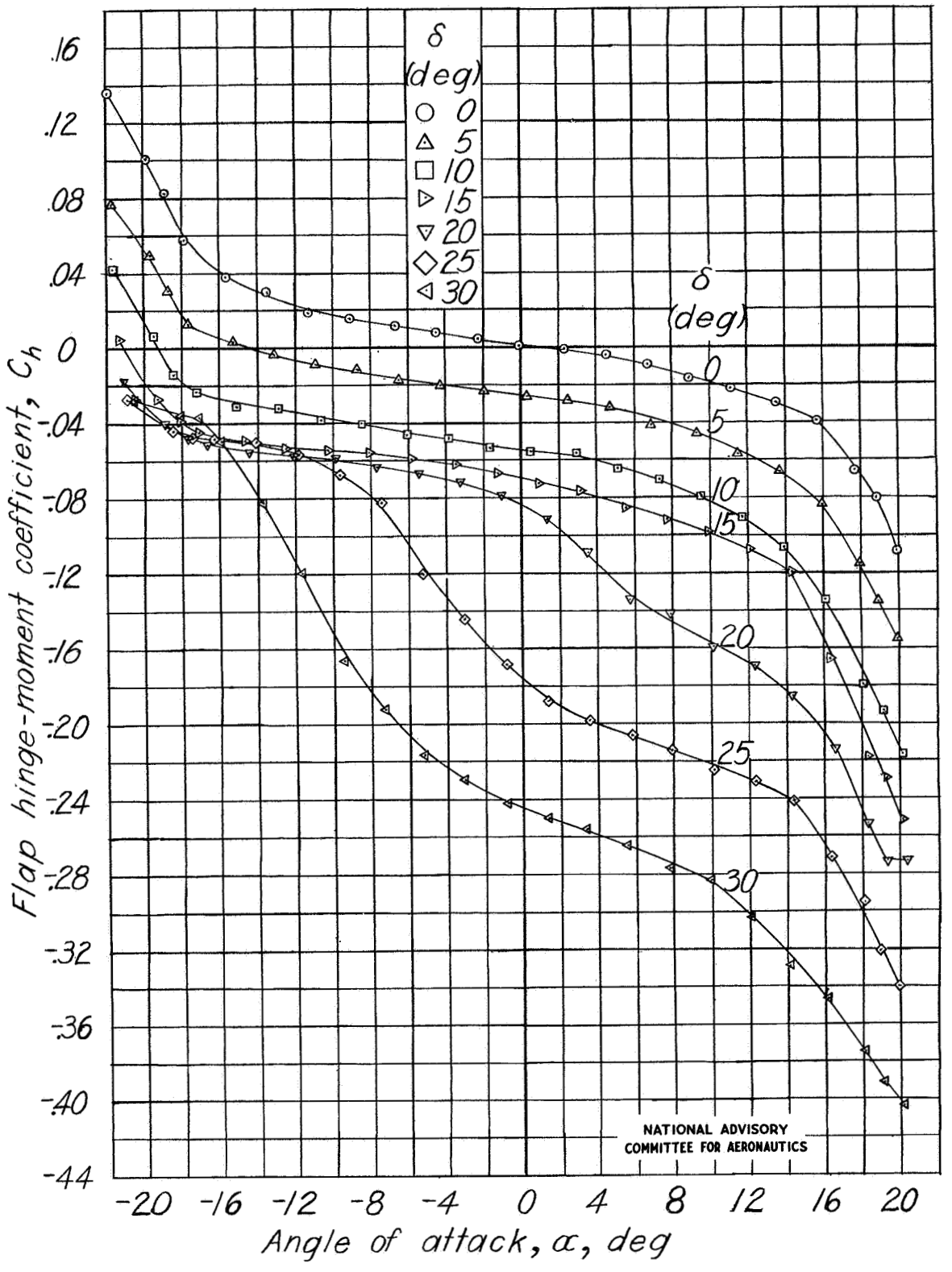

Figure 6.- Concluded. $0.35c_f$ overhang; $0.005c$ gap; $\phi = 111°$.

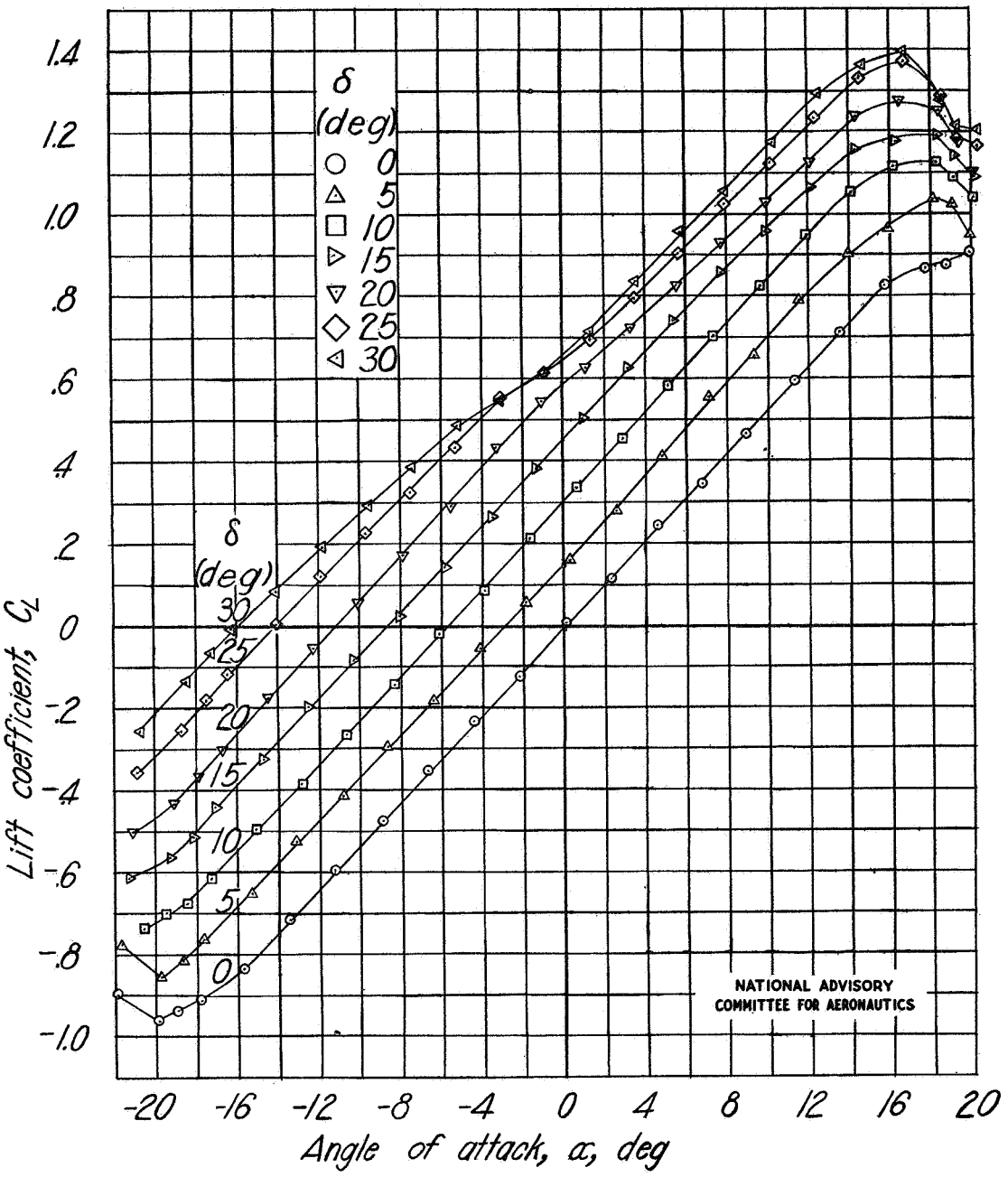

Figure 7.-Aerodynamic characteristics of a tapered semispan wing having a 0.30c beveled-trailing-edge plain flap. Sealed gap; $\phi = 19.8°$; $A = 3$.

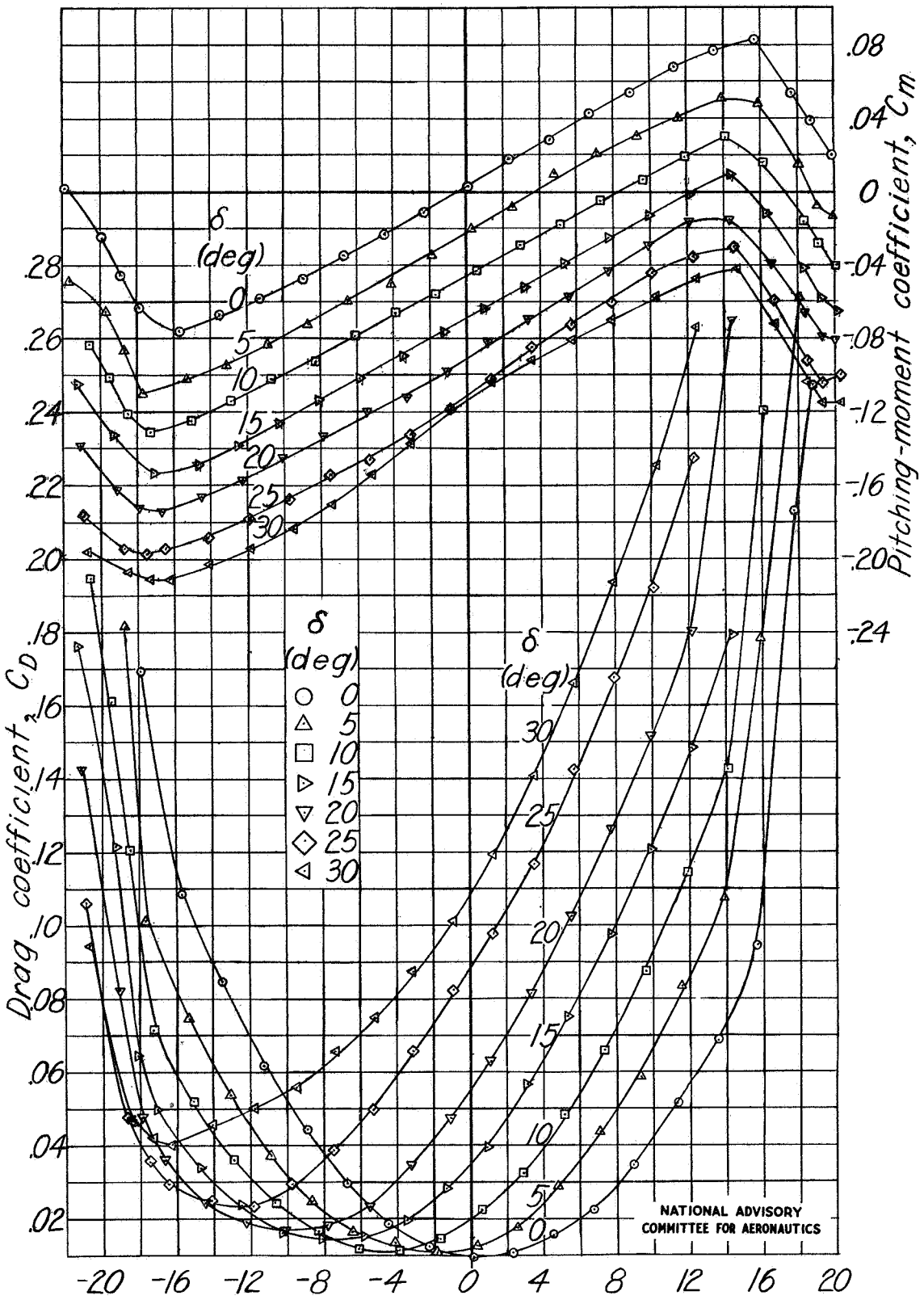

Figure 7.-Continued. Plain flap; sealed gap; ϕ=19.8°.

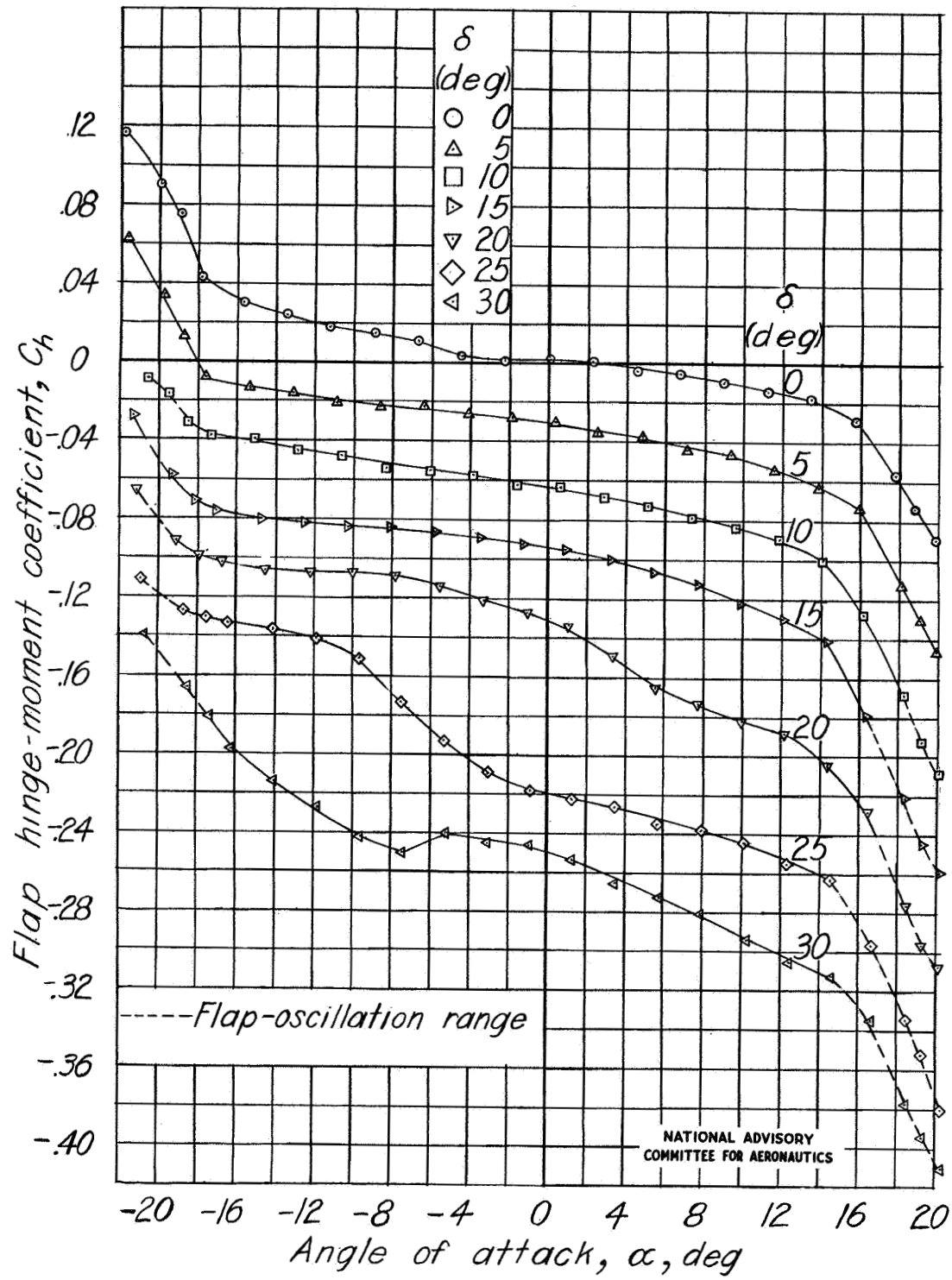

Figure 7.-Concluded. Plain flap; sealed gap; $\emptyset = 19.8°$.

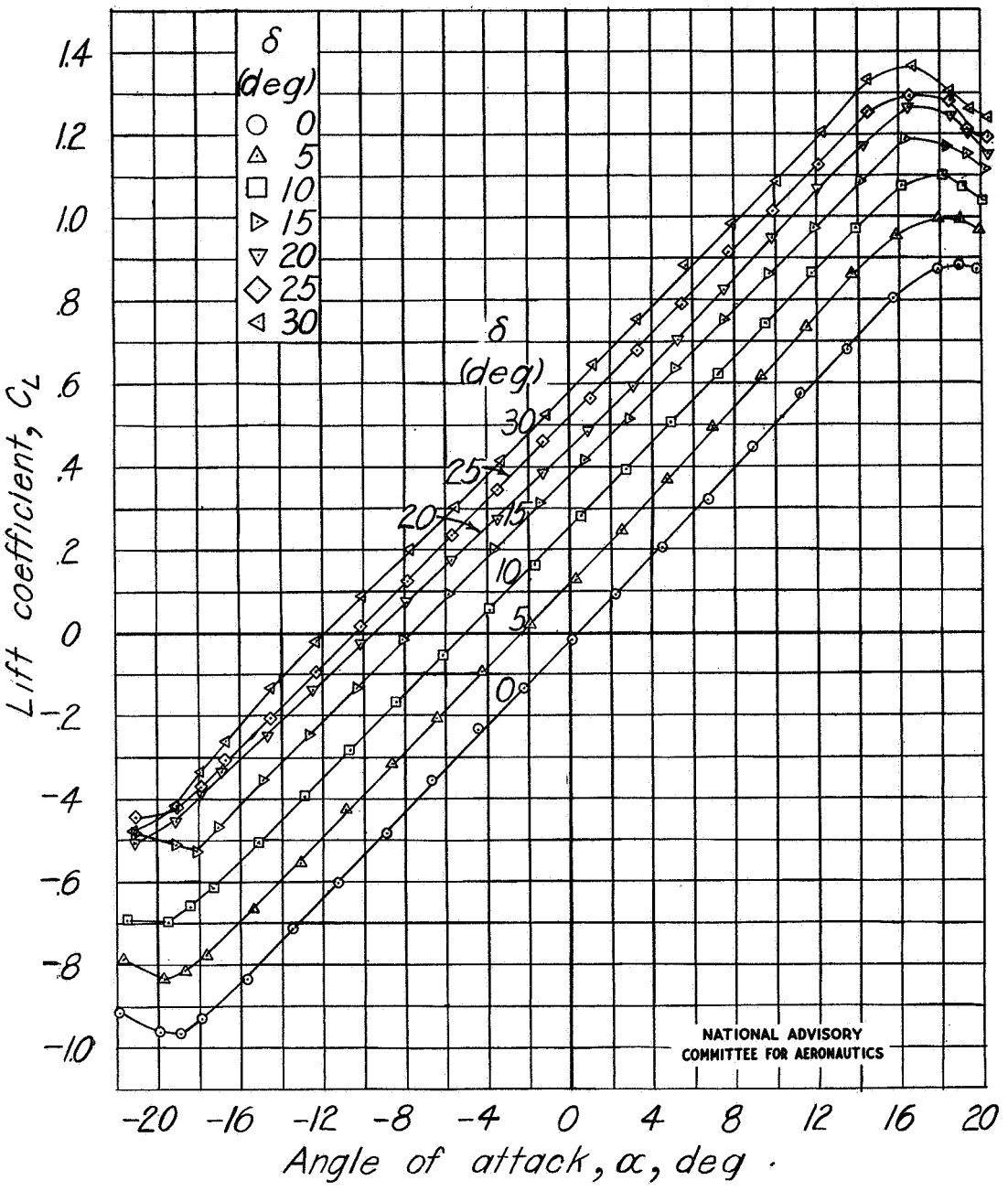

Figure 8.- Aerodynamic characteristics of a tapered semispan wing having a 0.30c beveled-trailing-edge plain flap. 0.005c gap; ϕ=19.8°; A=3.

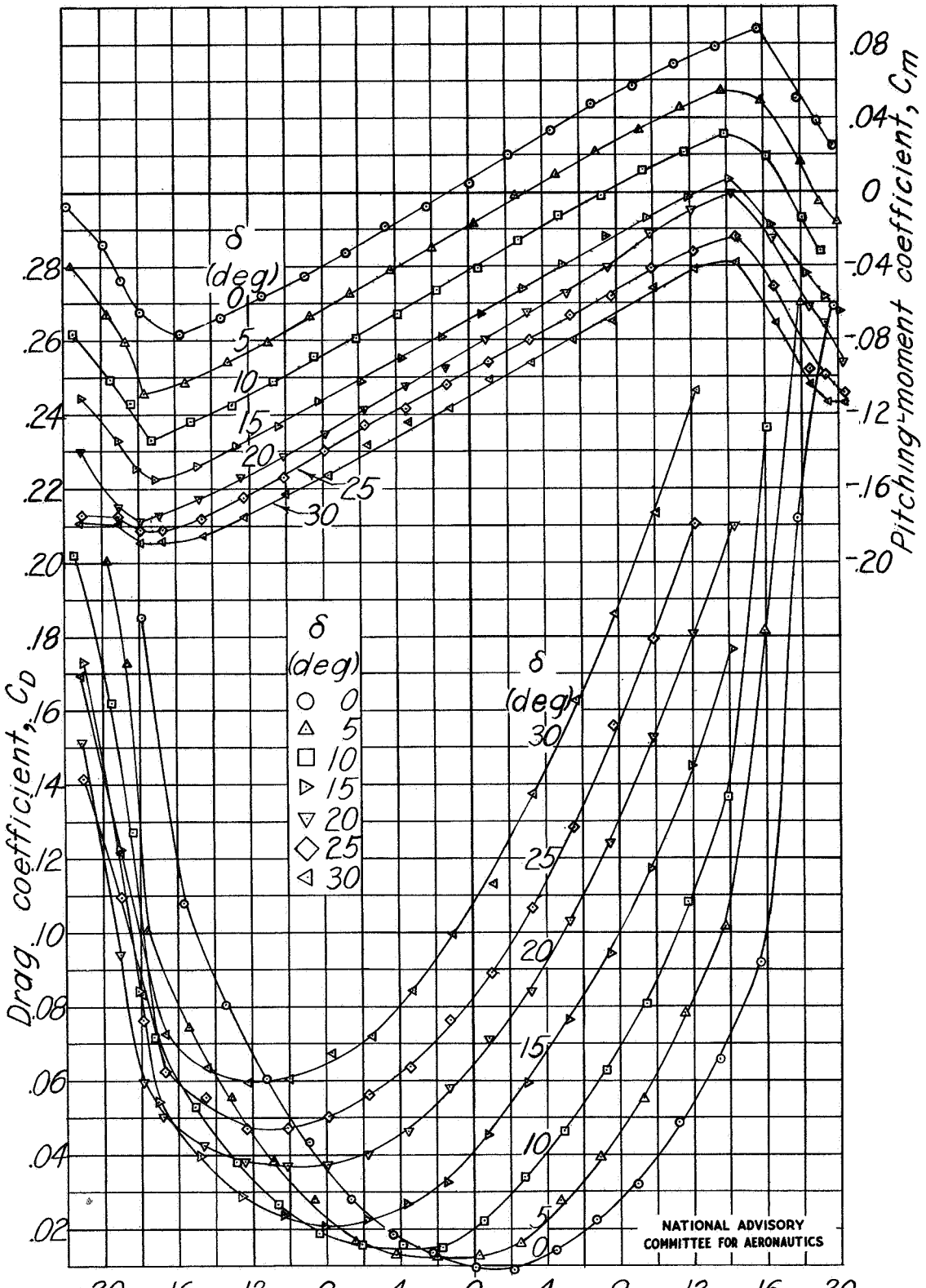

Figure 8 .-Continued. Plain flap; 0.005c gap; ϕ=19.8°.

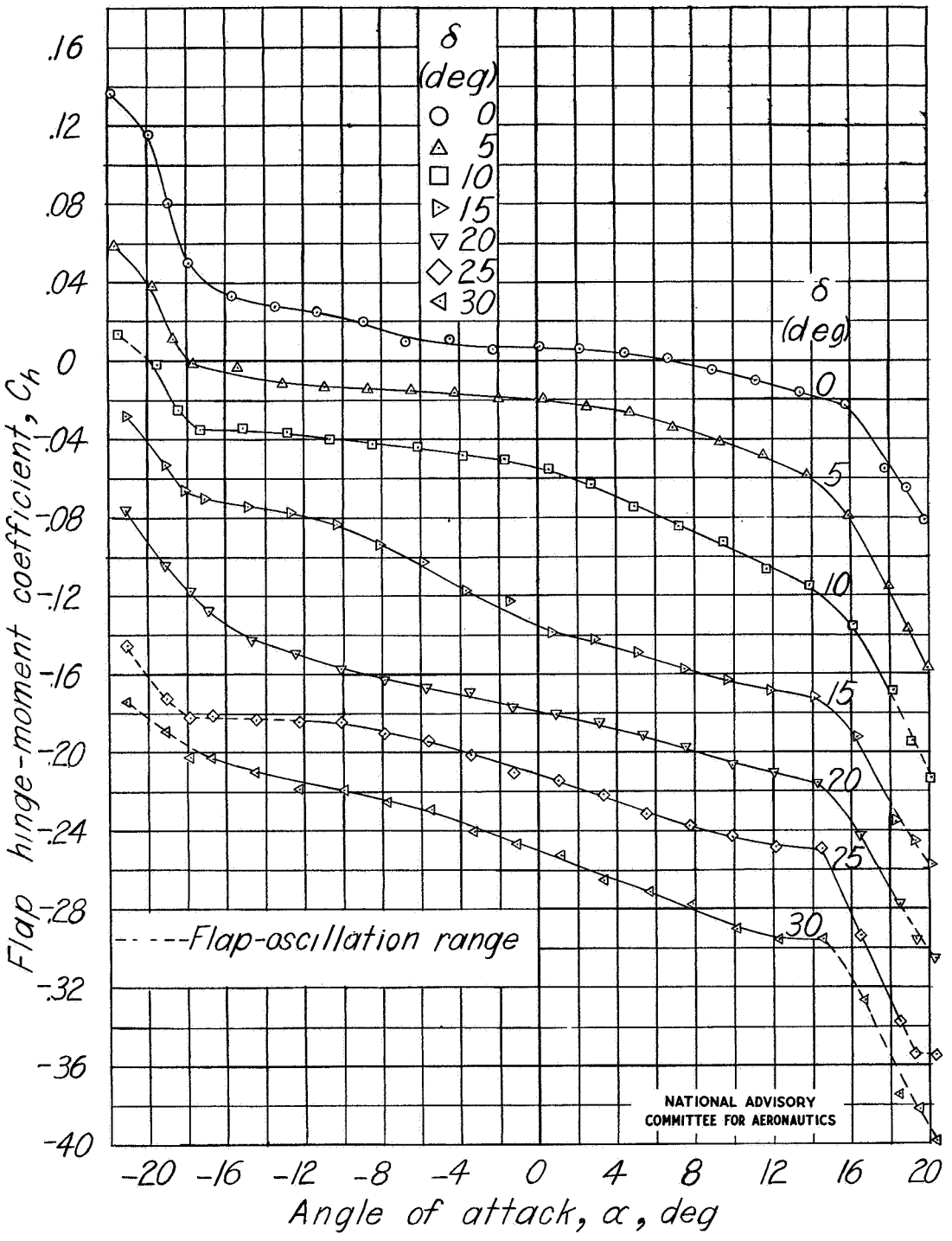

Figure 8.- Concluded. Plain flap; 0.005c gap; $\phi = 19.8°$.

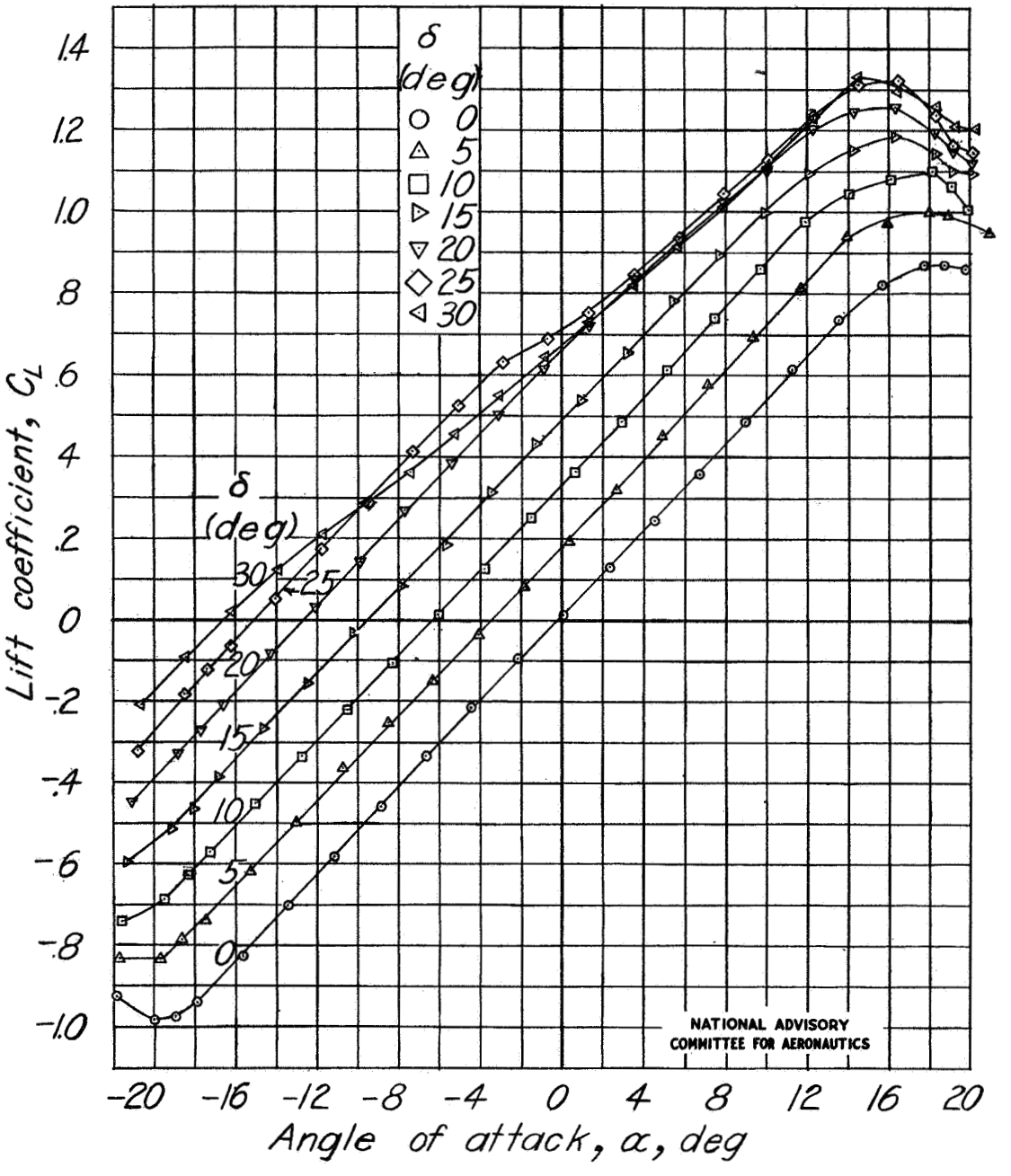

Figure 9.-Aerodynamic characteristics of a tapered semispan wing having a 0.30c beveled-trailing-edge flap with a $0.35c_f$ elliptical overhang. Sealed gap; $\phi=19.8°$; $A=3$.

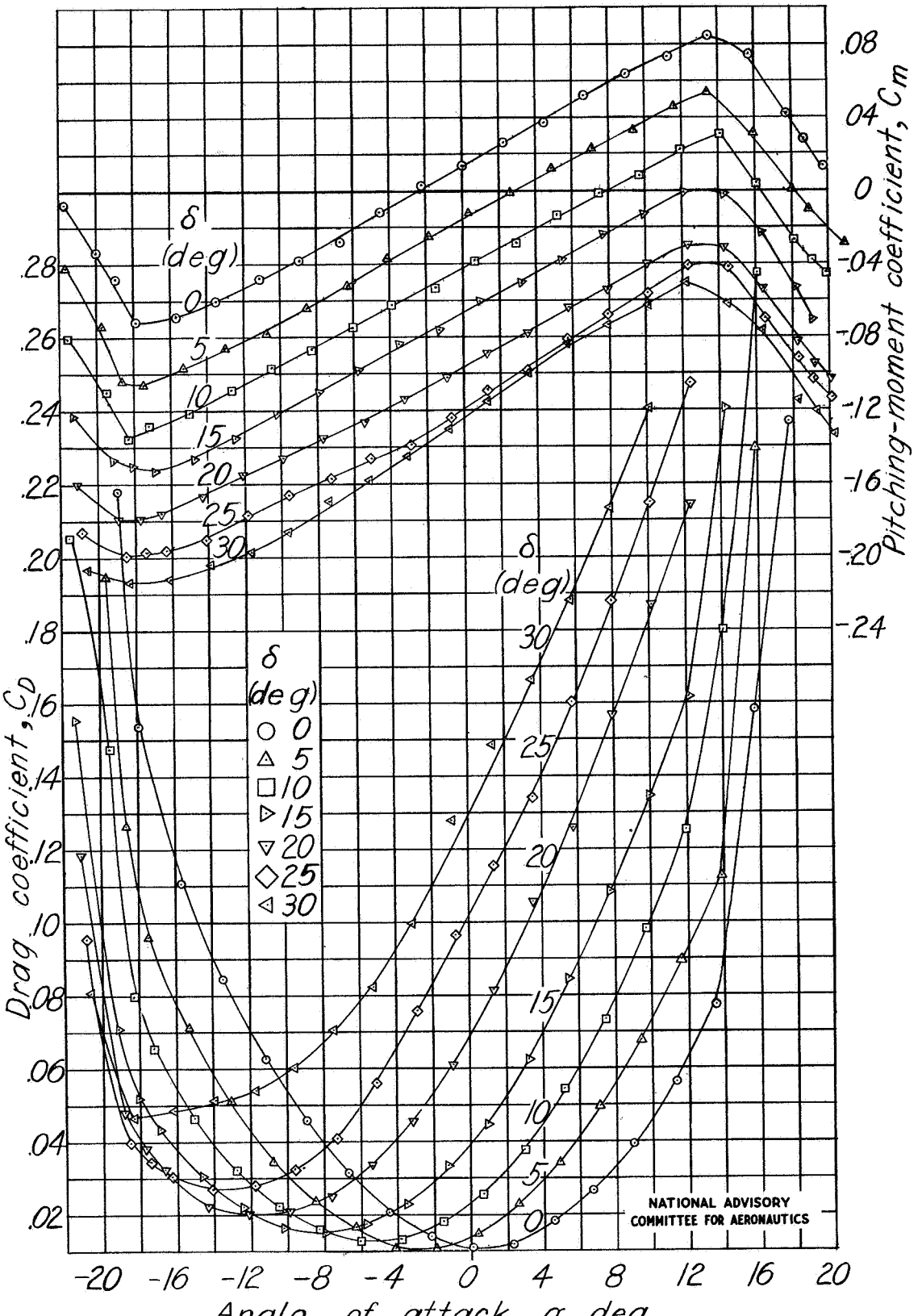

Figure 9.-Continued. 0.35c_f overhang; sealed gap; ϕ=19.8°

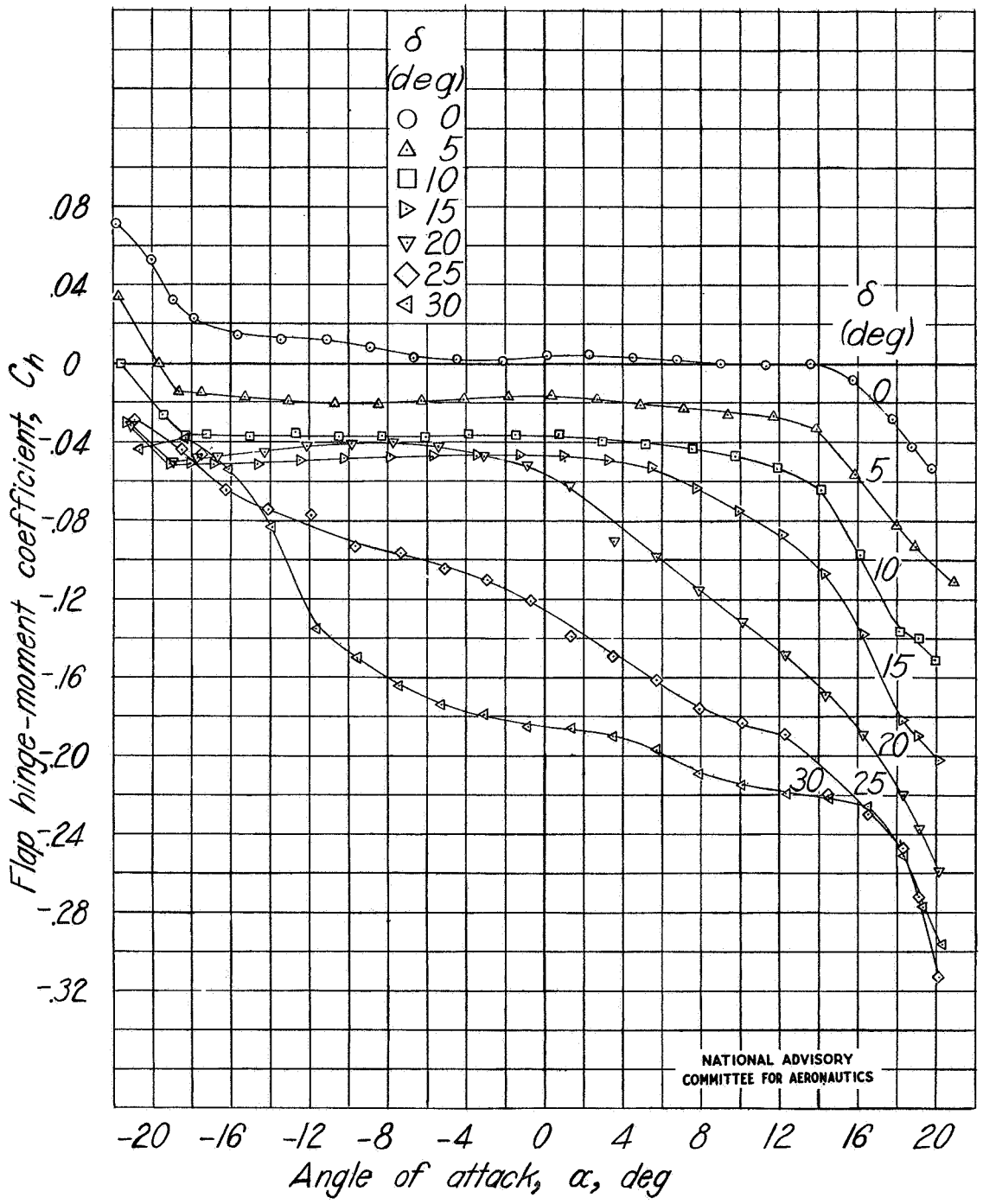

Figure 9 .- Concluded. 0.35c_f overhang; sealed gap; $\phi = 19.8°$.

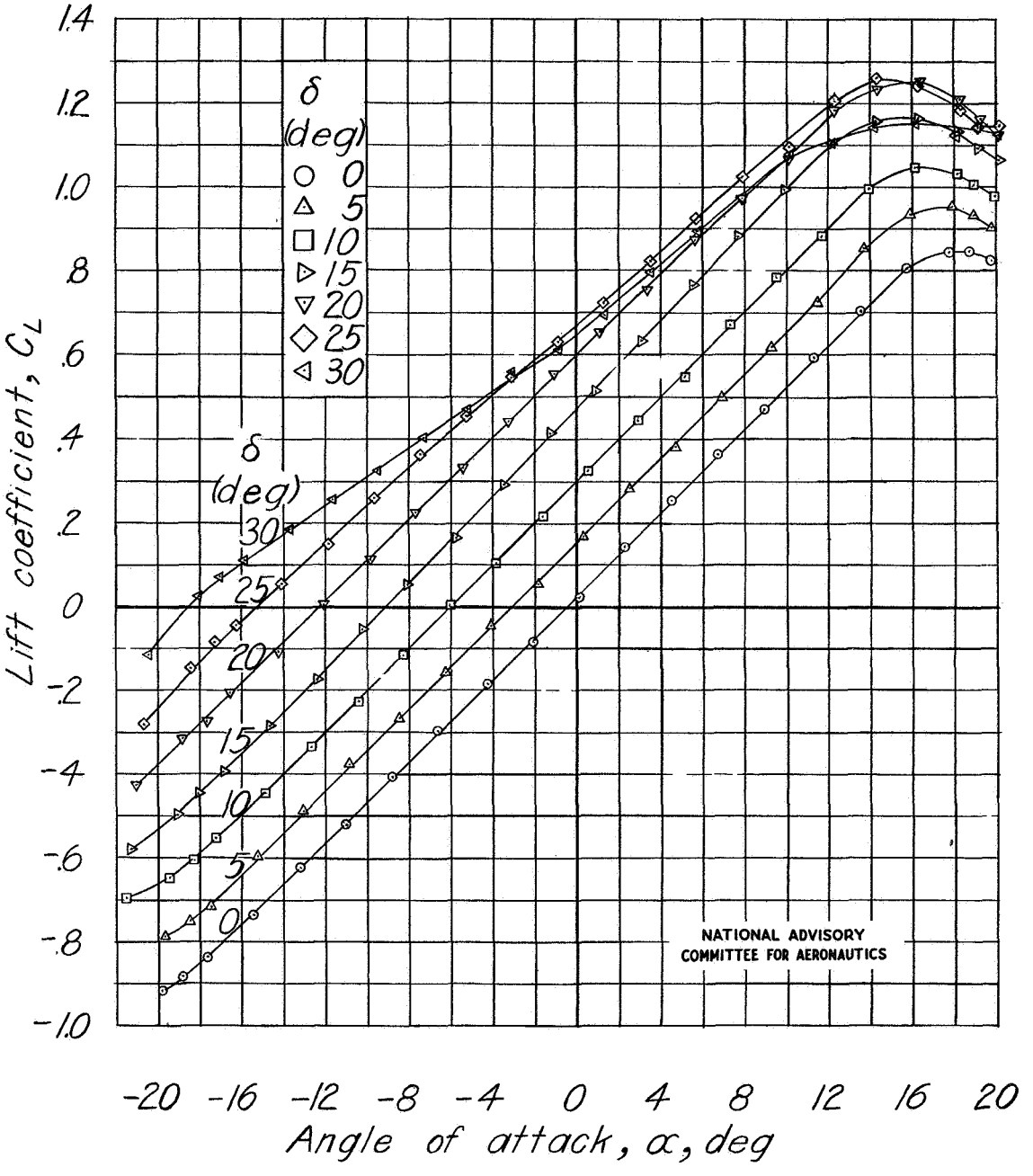

Figure 10.-Aerodynamic characteristics of a tapered semispan wing having a 0.30c beveled-trailing-edge flap with a $0.35c_f$ elliptical overhang. 0.005c gap; $\Phi = 19.8°$; $A = 3$.

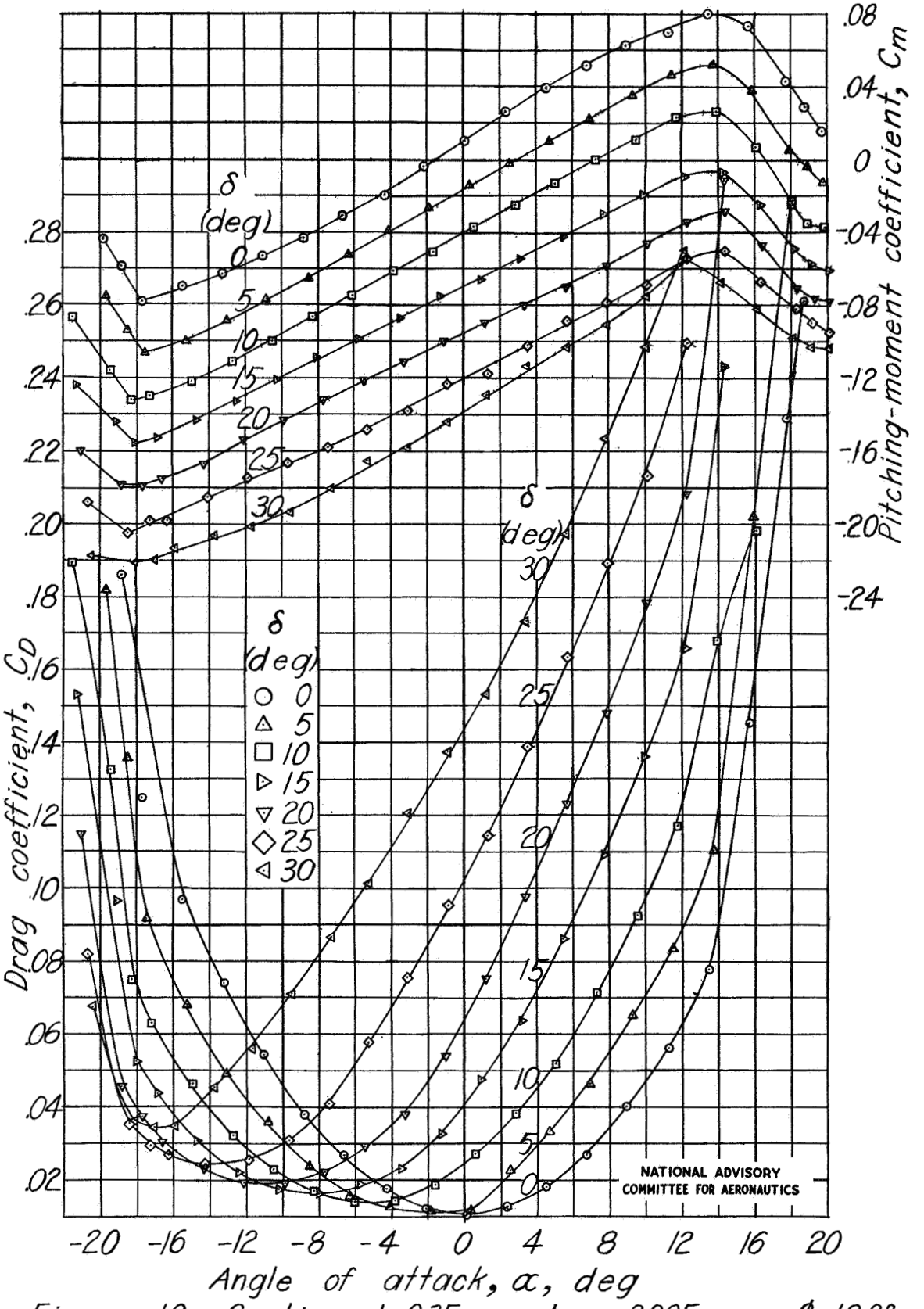

Figure 10.- Continued. $0.35c_f$ overhang; $0.005c$ gap; $\phi = 19.8°$.

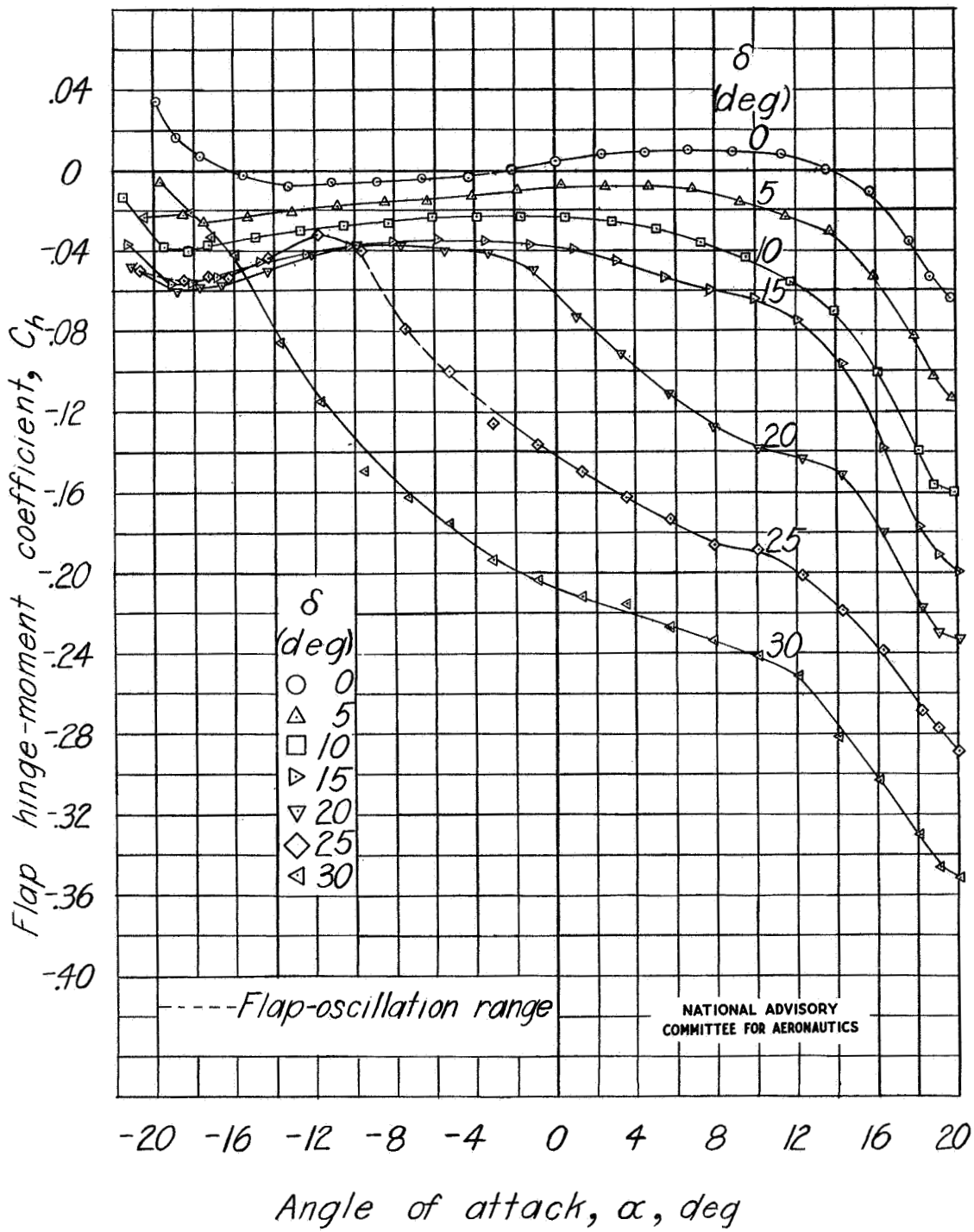

Figure 10.- Concluded. $0.35c_f$ overhang; 0.005c gap; ϕ=19.8°.

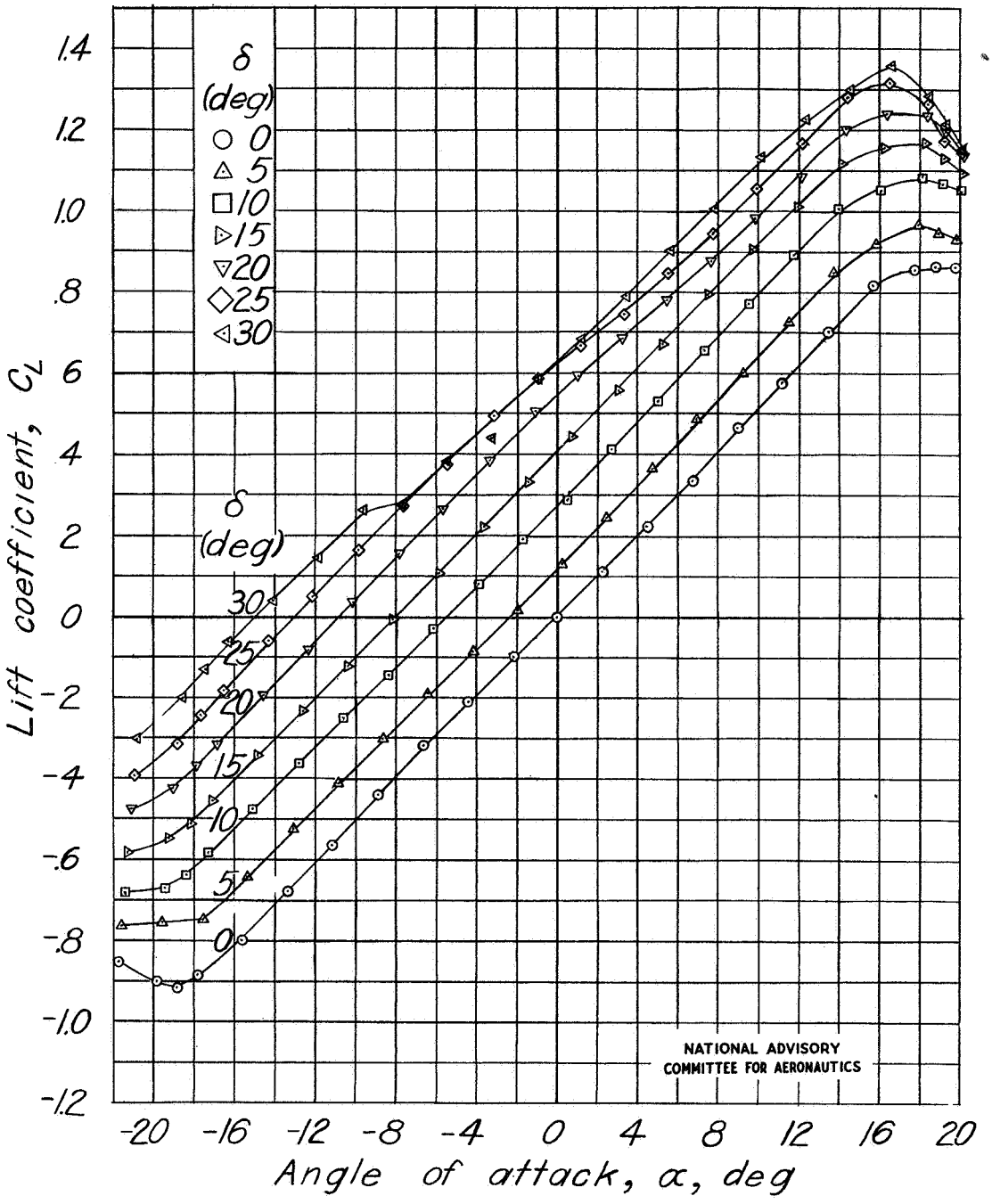

Figure 11.- Aerodynamic characteristics of a tapered semispan wing having a 0.30c beveled-trailing-edge plain flap. Sealed gap; ϕ=29.6°; A=3.

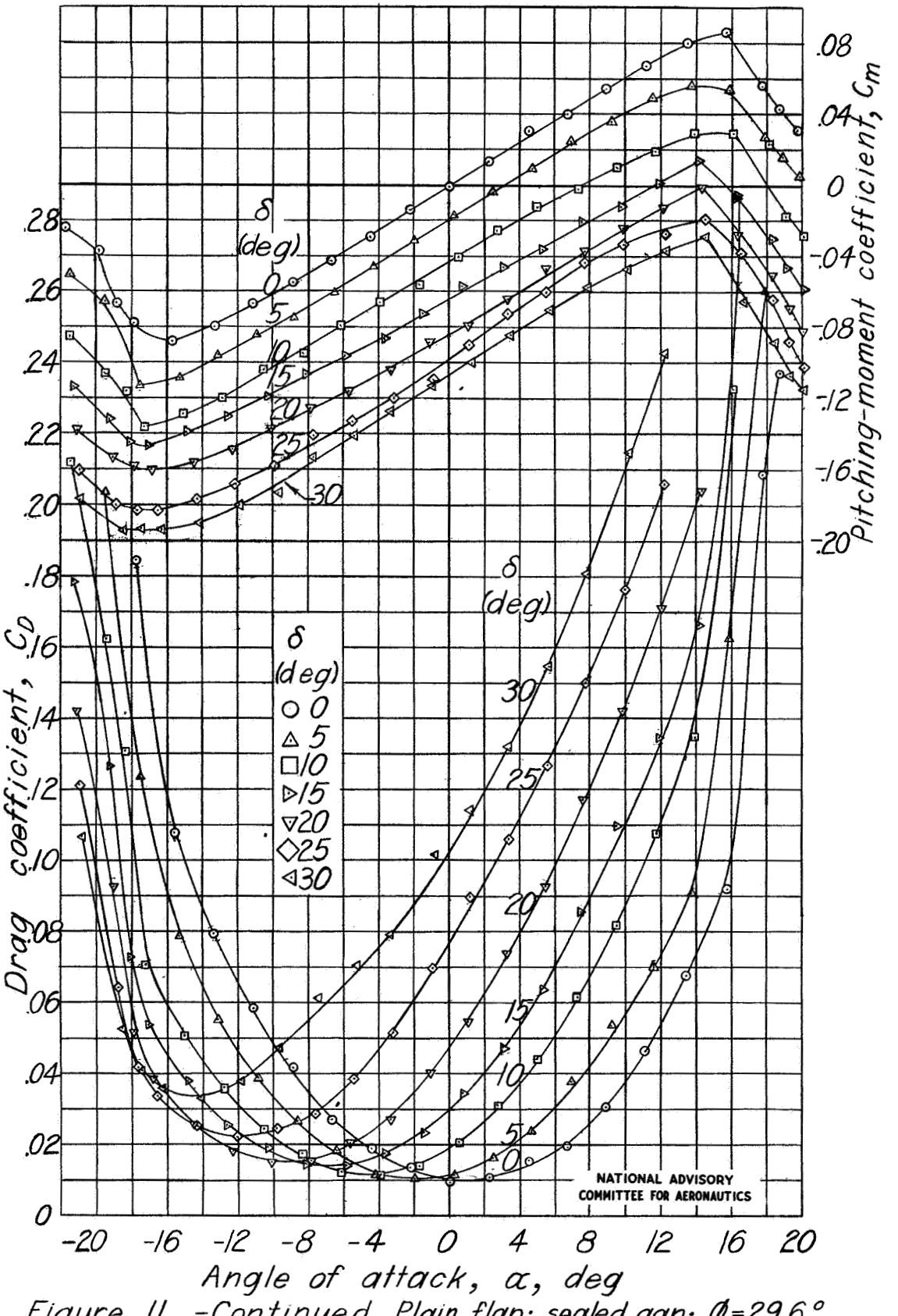

Figure 11 .-Continued. Plain flap; sealed gap; $\emptyset = 29.6°$.

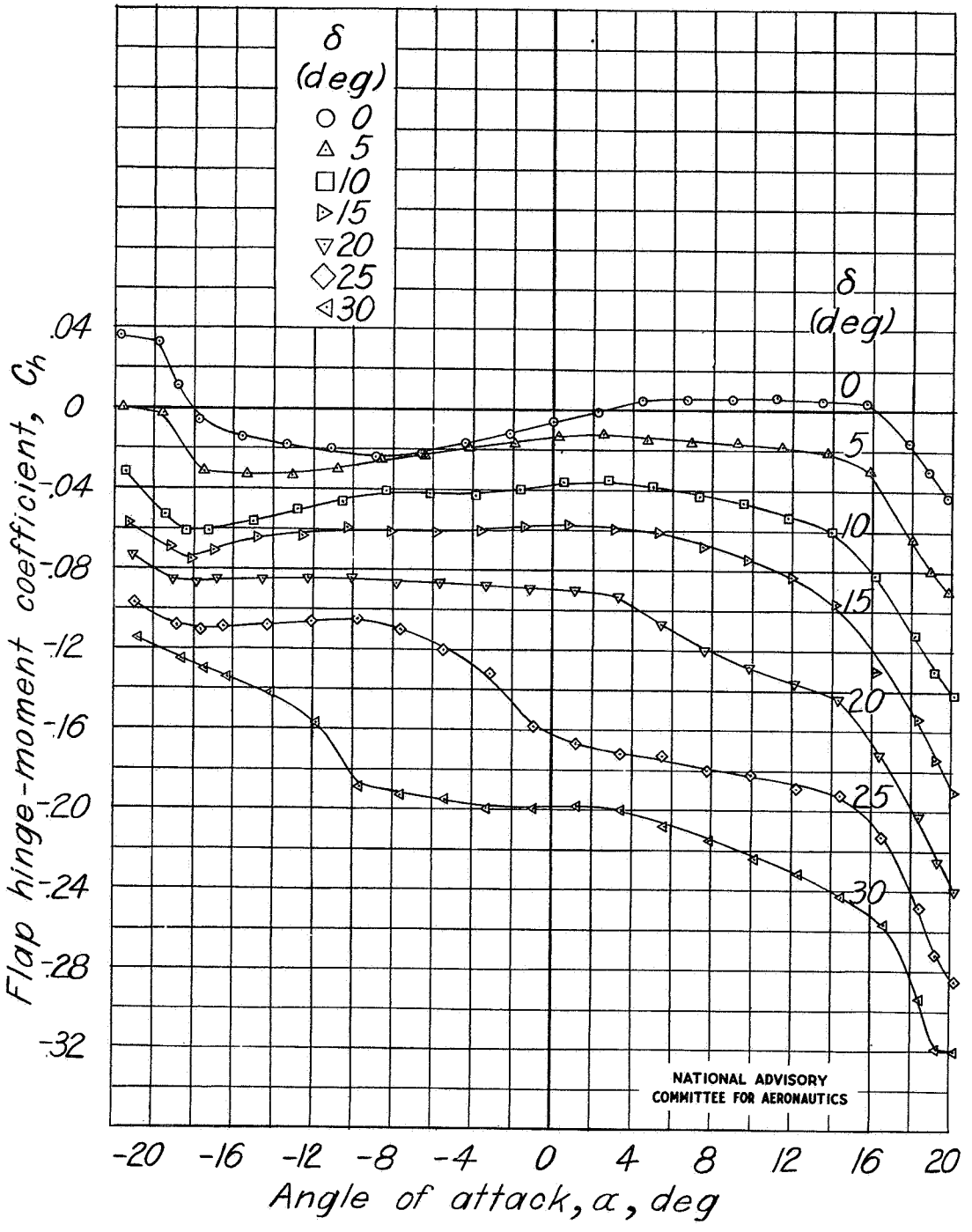

Figure 11.- Concluded. Plain flap; sealed gap; $\emptyset = 29.6°$.

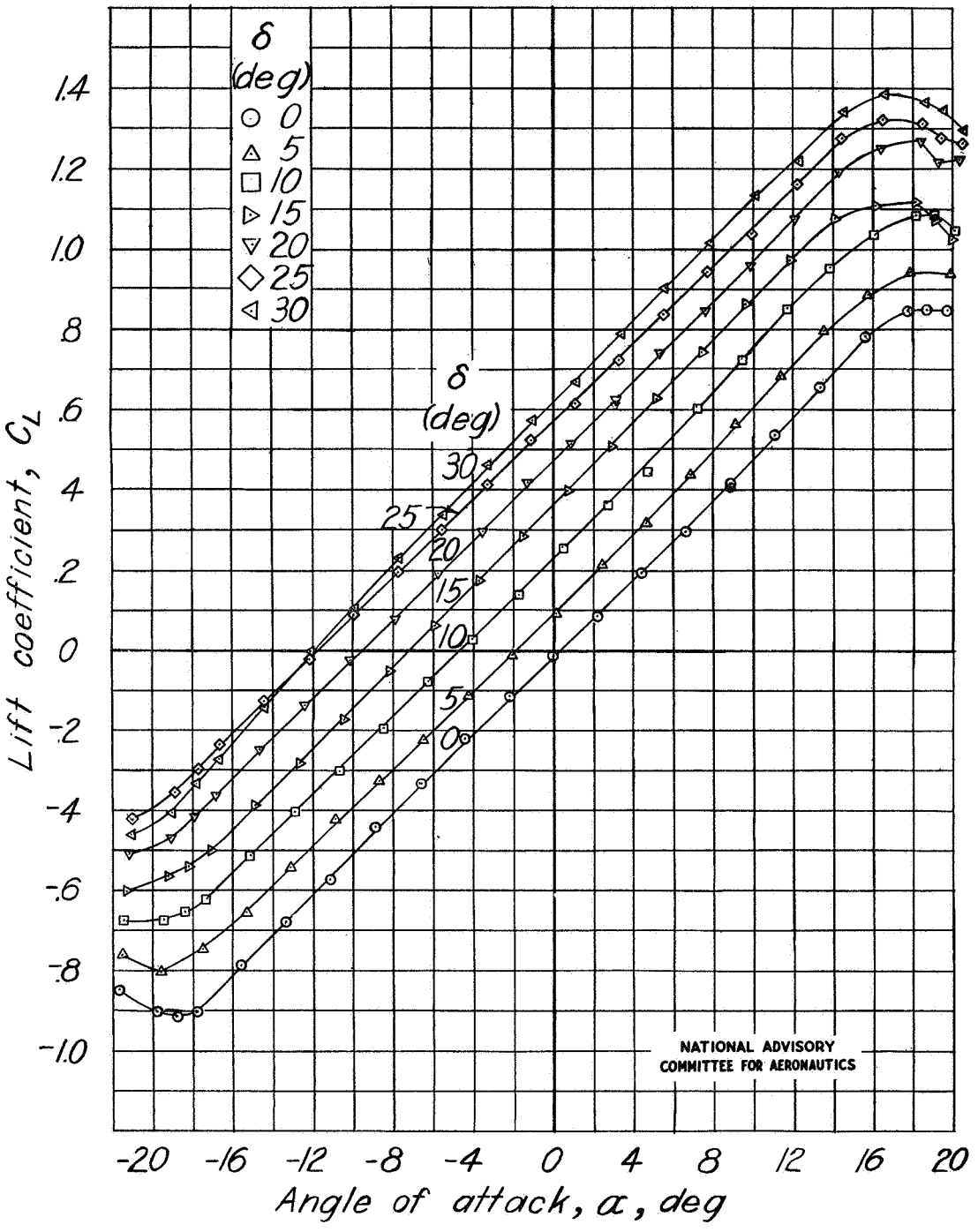

Figure 12.- Aerodynamic characteristics of a tapered semispan wing having a 0.30c beveled-trailing-edge plain flap. 0.005c gap; $\phi = 29.6°$ $A = 3$.

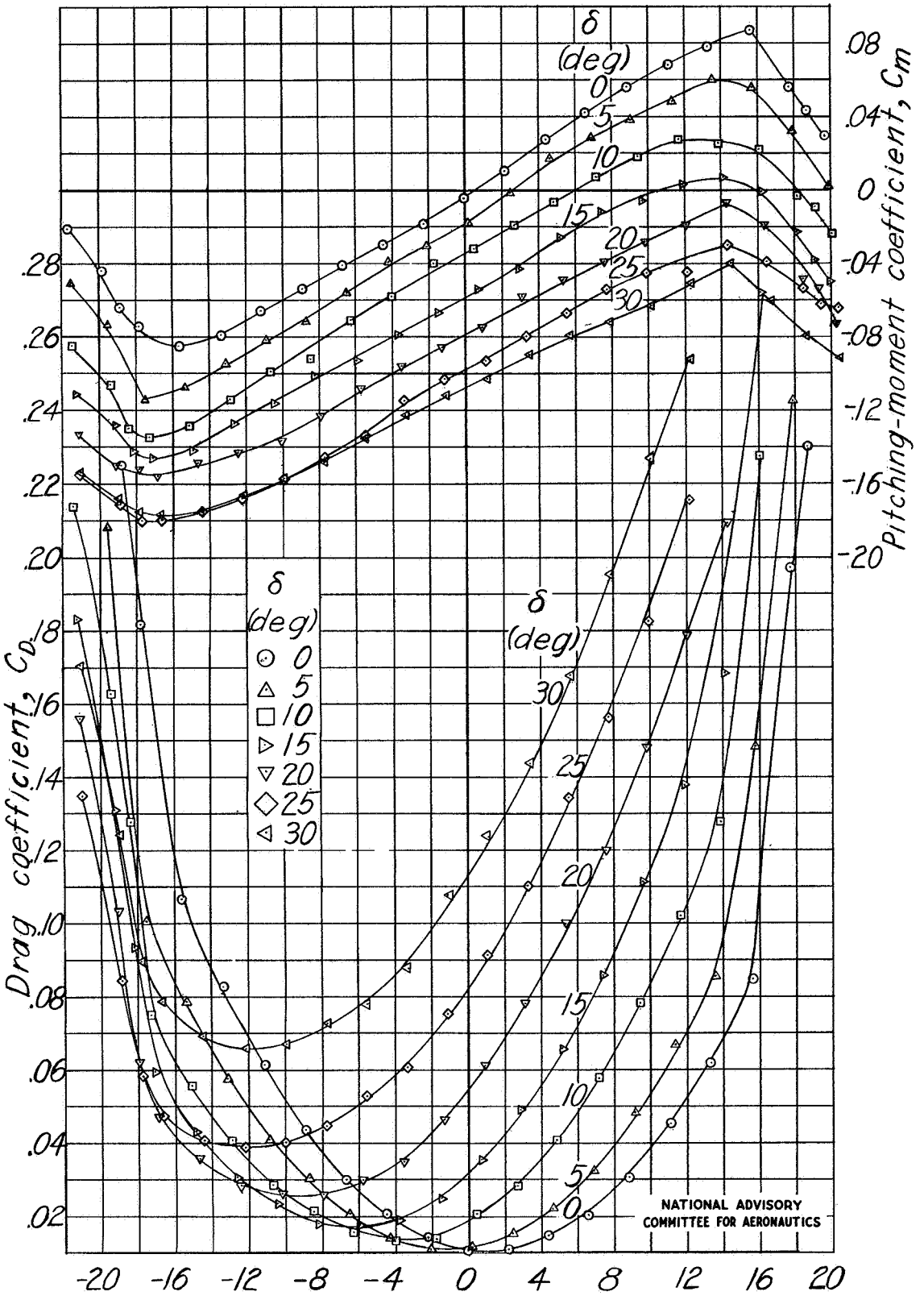

Figure 12.- Continued. Plain flap; 0.005c gap; $\phi = 29.6°$.

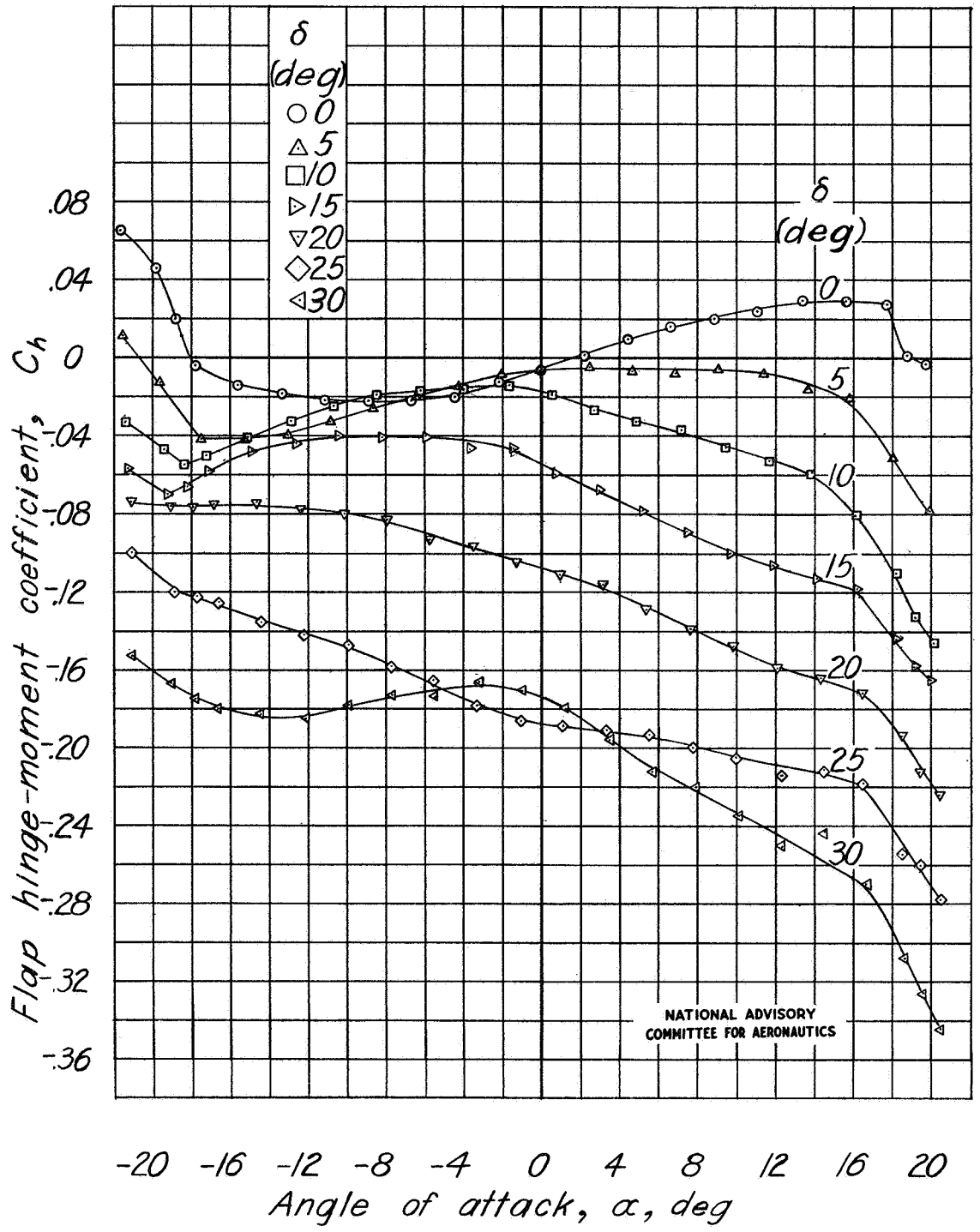

Figure 12.-Concluded. Plain flap; 0.005c gap; $\emptyset$=29.6°.

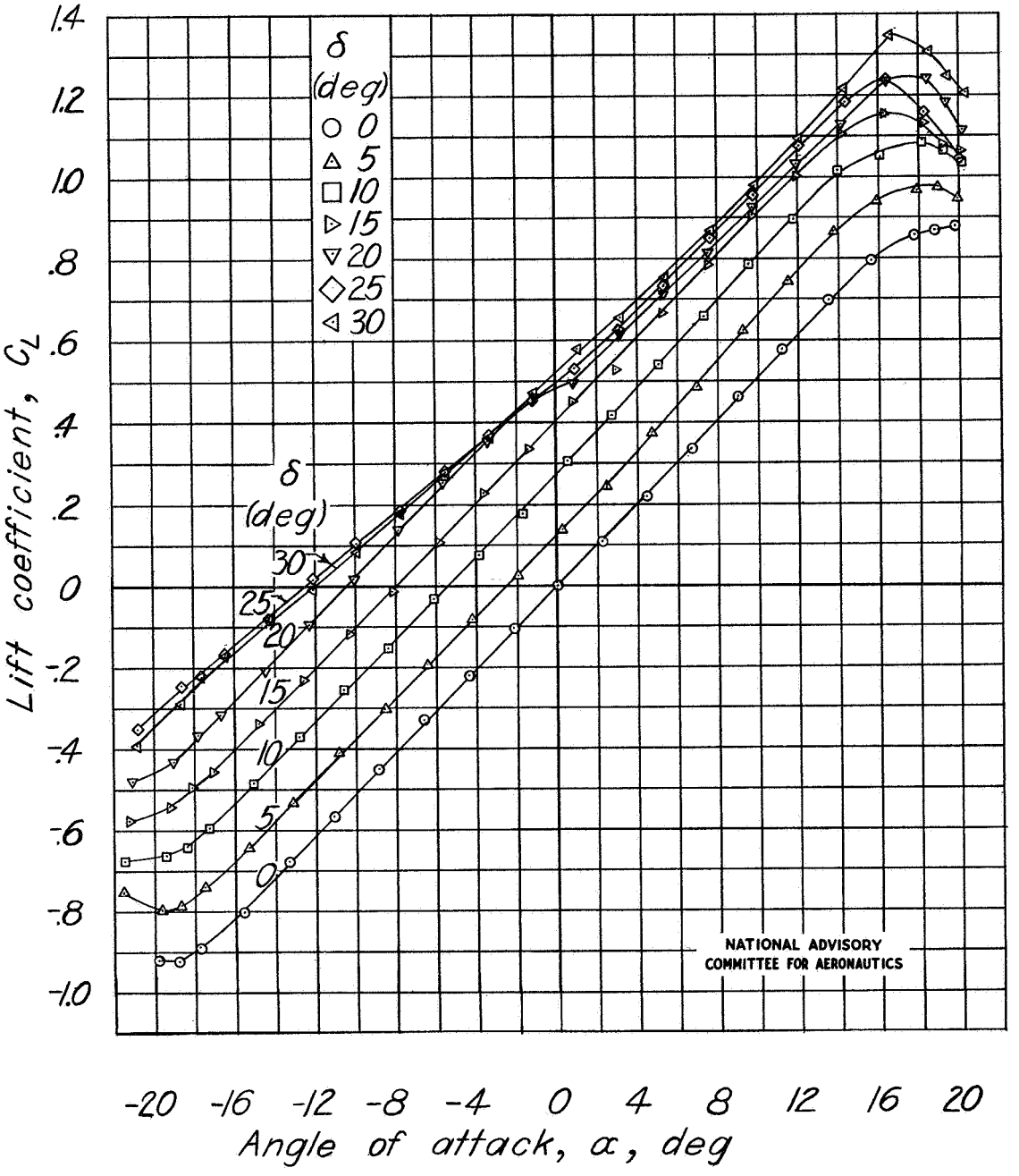

Figure 13.-Aerodynamic characteristics of a tapered semispan wing having a 0.30c beveled-trailing-edge flap with a 0.35c_f elliptical overhang. Sealed gap; $\Phi = 29.6^\circ$; A = 3.

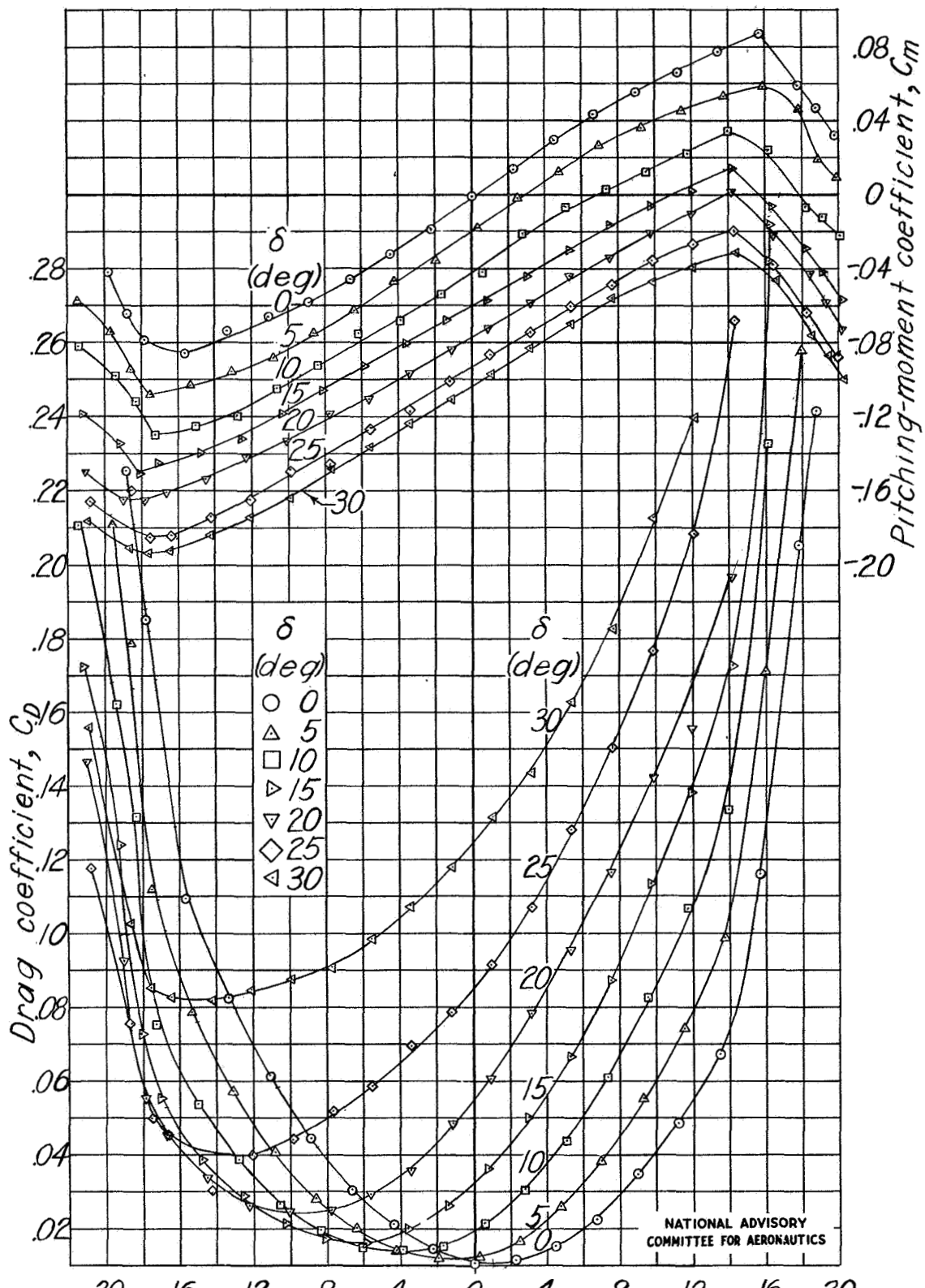

Figure 13.-Continued. 0.35c_f overhang; sealed gap; ϕ=29.6°.

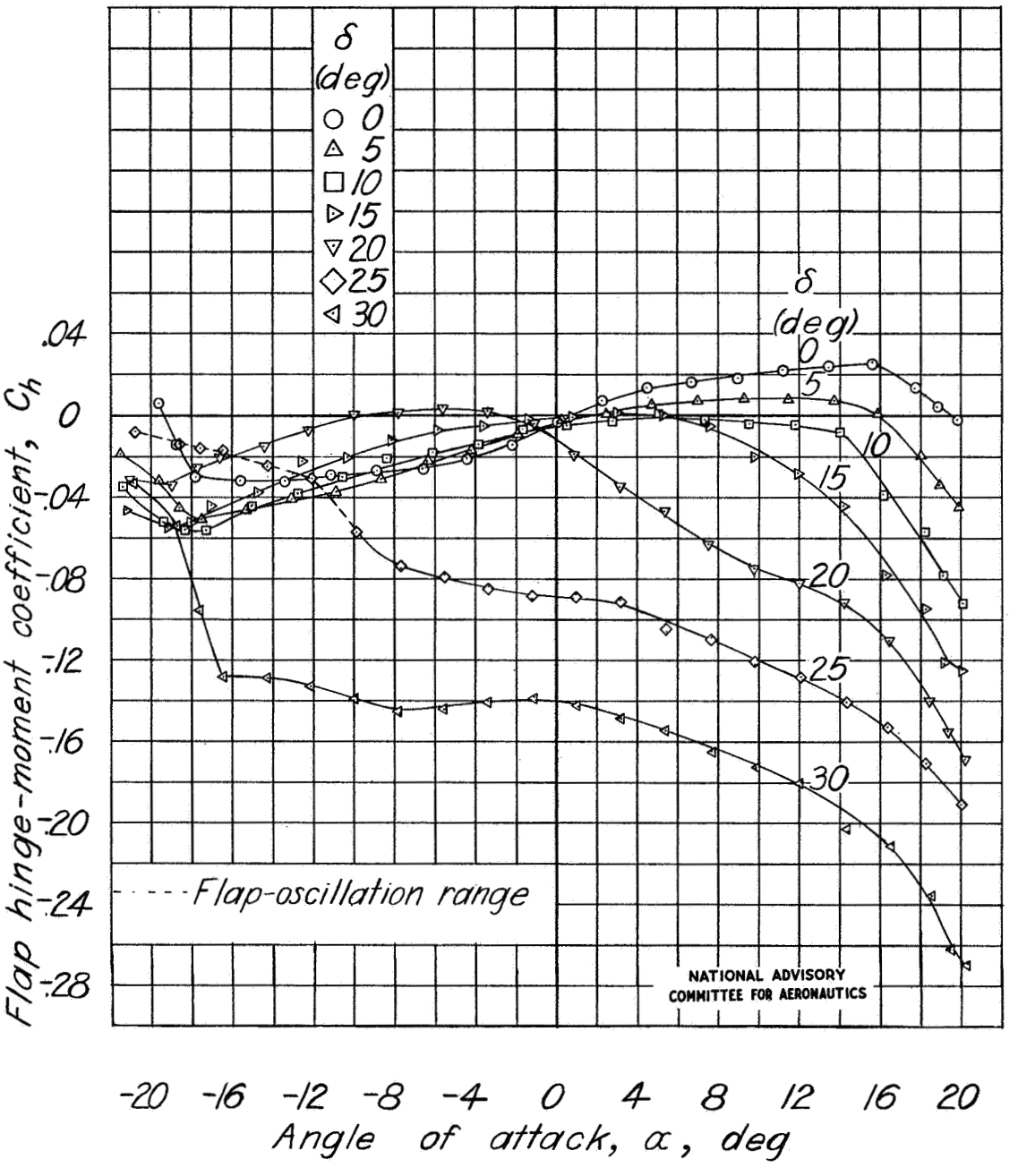

Figure 13.- Concluded. 0.35c_f overhang; sealed gap; $\emptyset$=29.6°

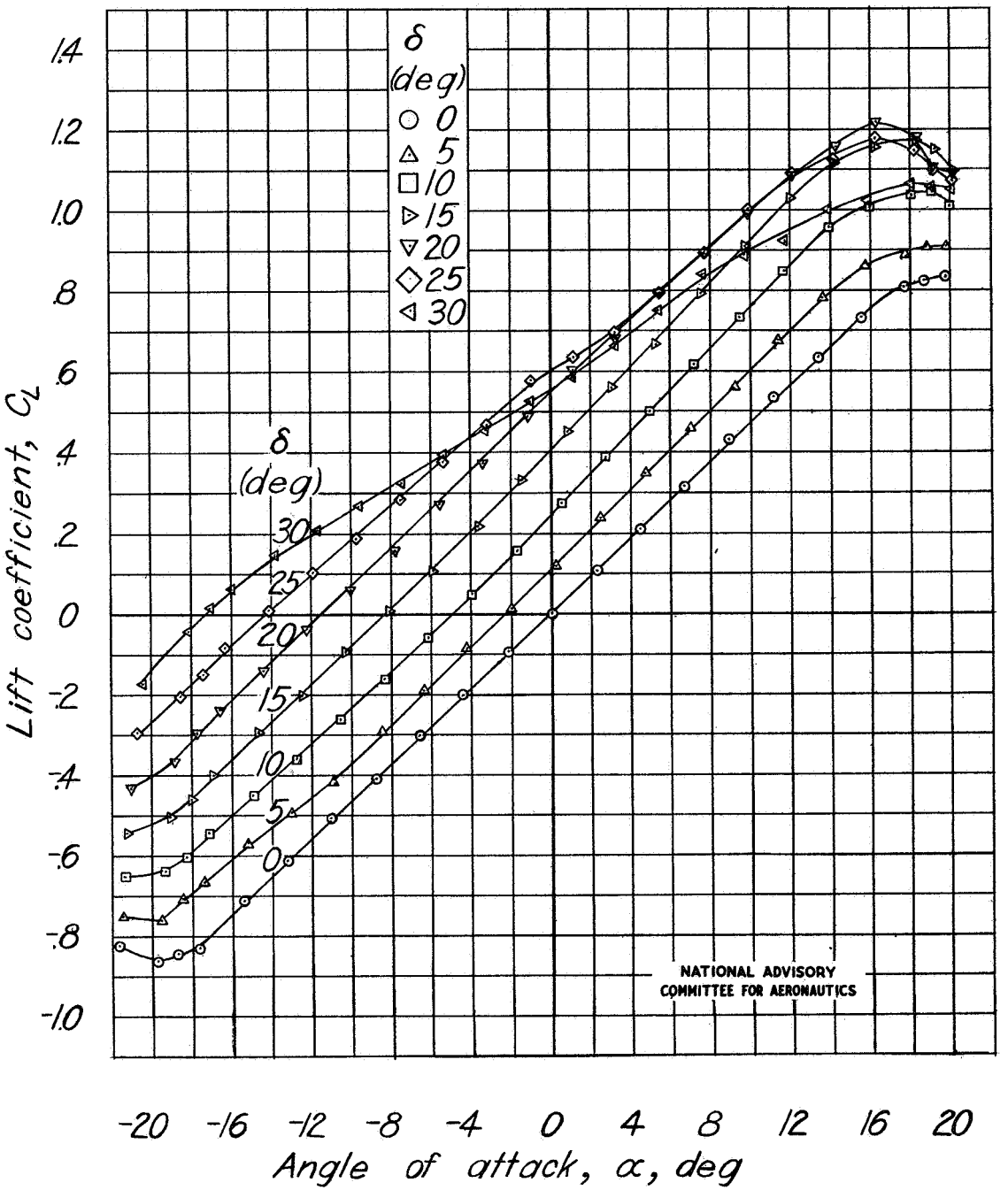

Figure 14.-Aerodynamic characteristics of a tapered semispan wing having a 0.30c beveled-trailing-edge flap with a $0.35c_f$ elliptical overhang. 0.005c gap; $\phi = 29.6°$; A = 3.

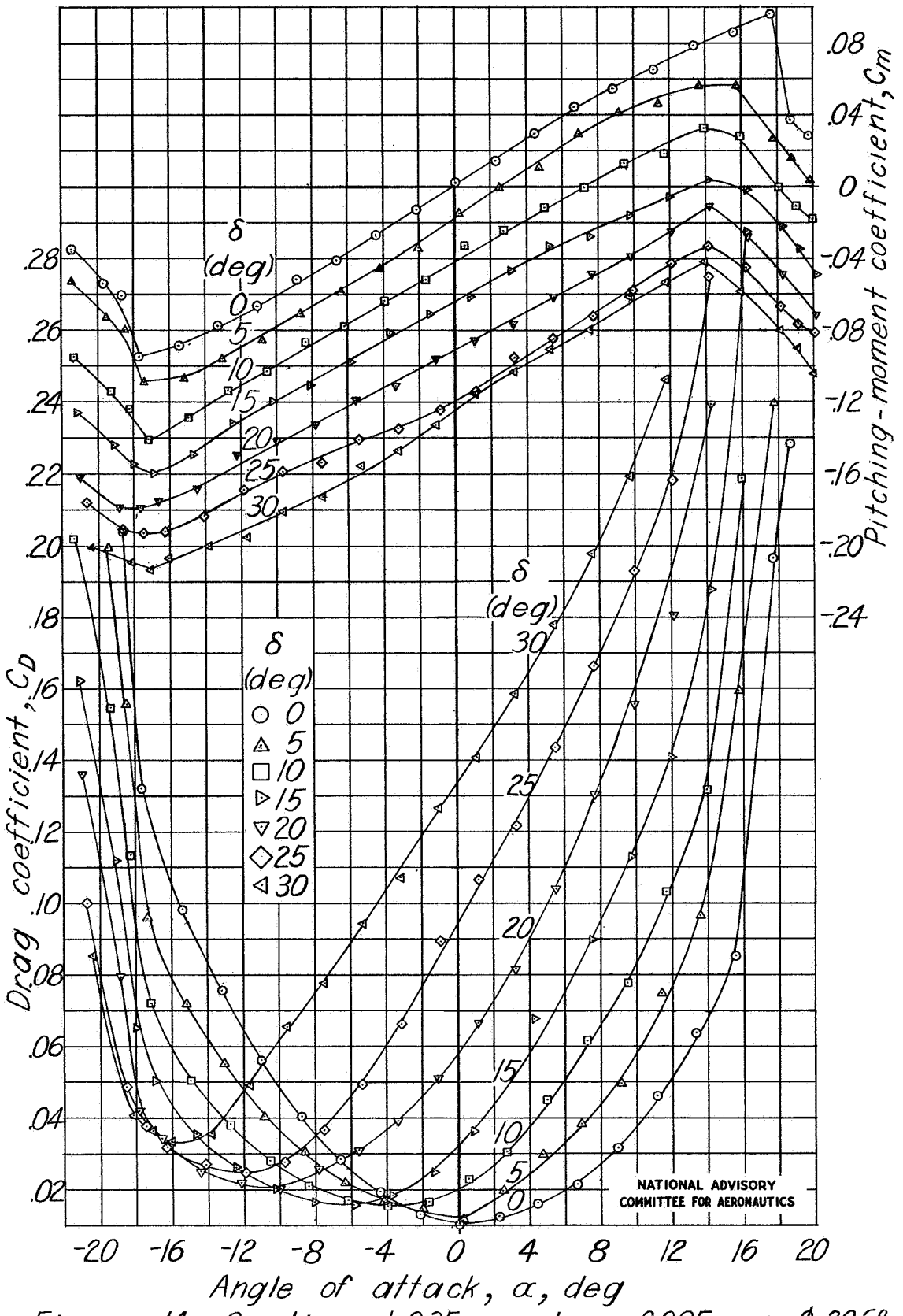

Figure 14.- Continued. 0.35c_f overhang; 0.005c gap; ϕ=29.6°.

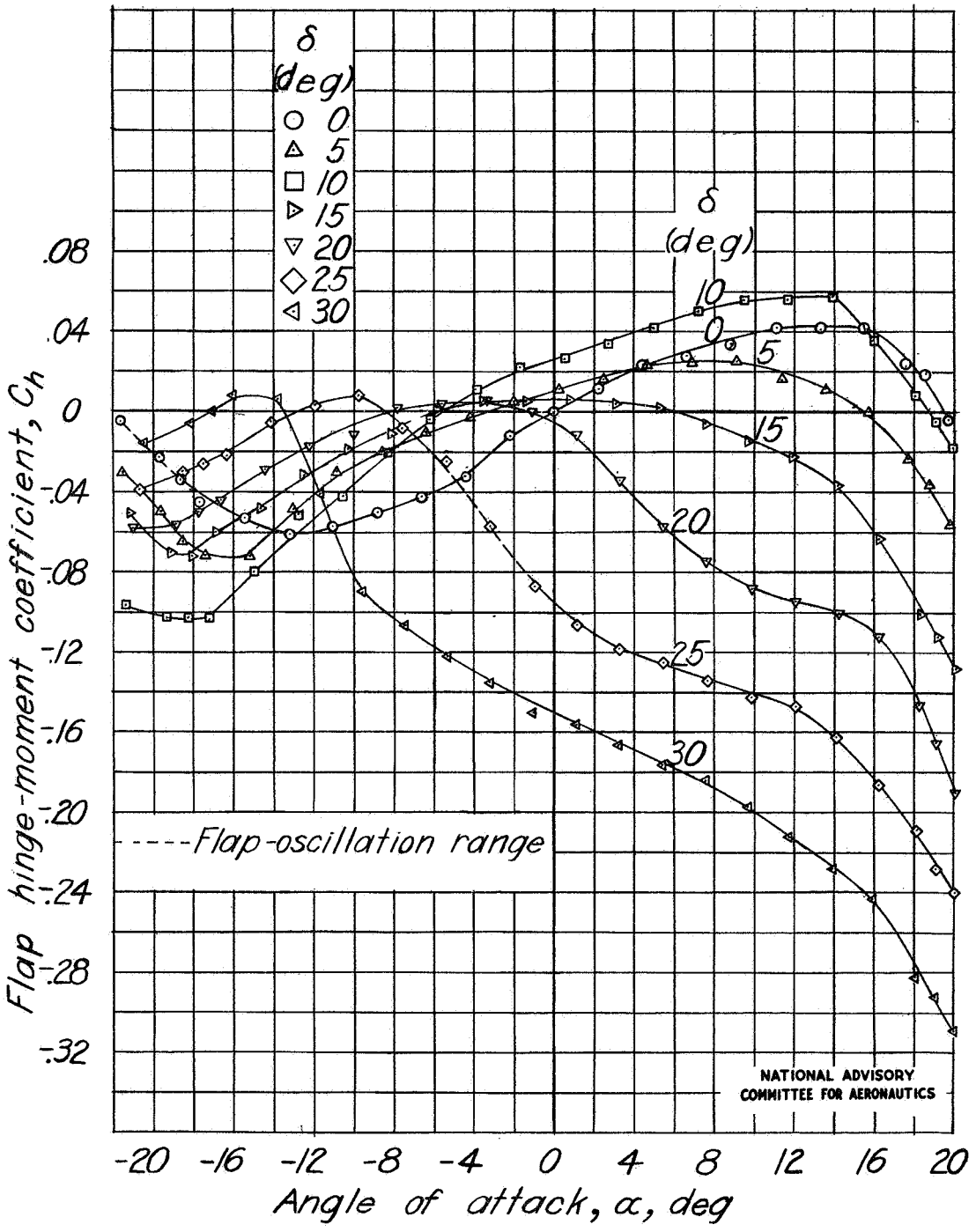

Figure 14.-Concluded. $0.35c_f$ overhang; 0.005c gap; ϕ=29.6°

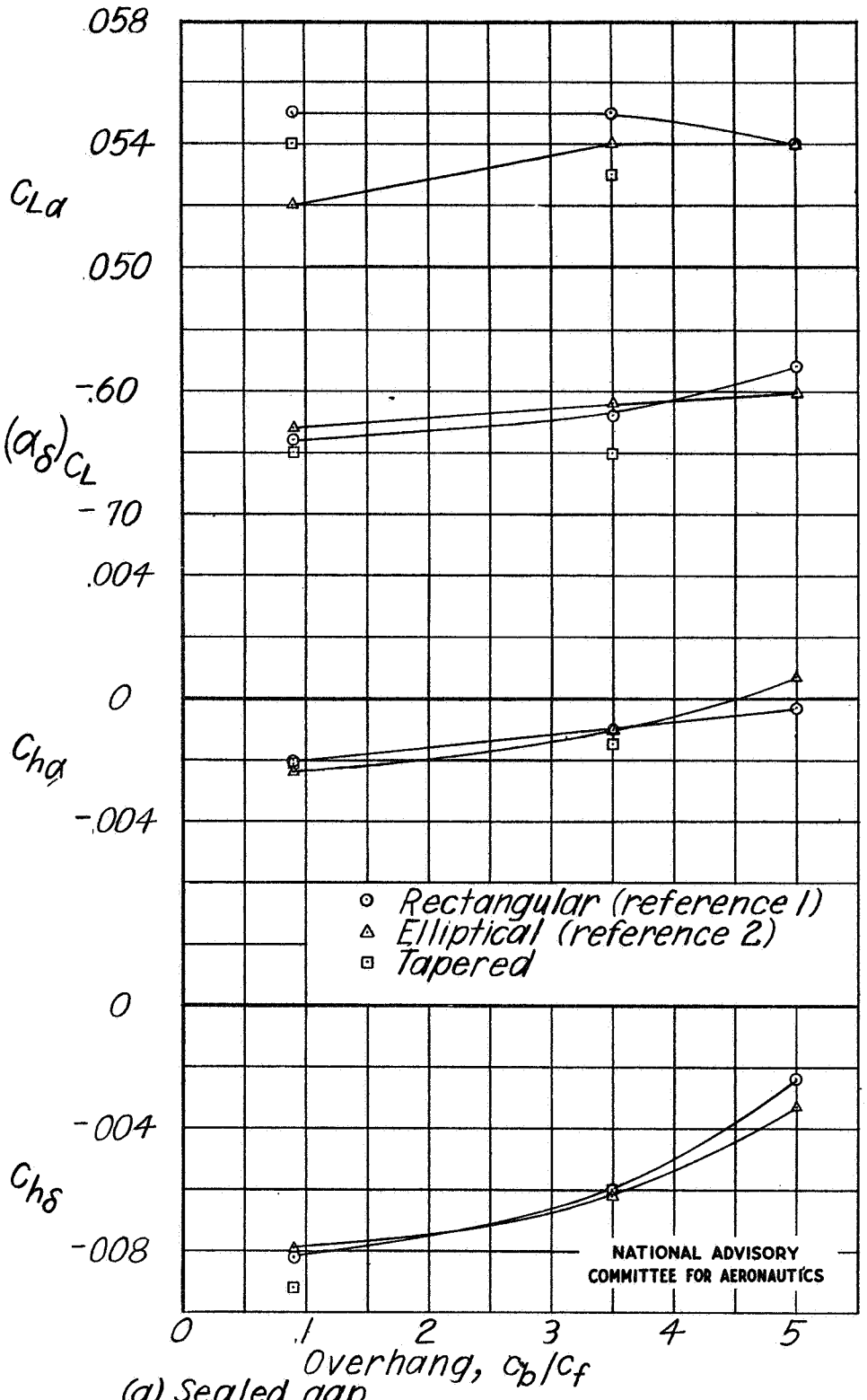

(a) Sealed gap.

Figure 15.-Comparison of the parameter values on rectangular, elliptical, and tapered semispan wings. (c_f = 0.30c on rectangular and tapered wings; flap area is 0.30 times wing area on elliptical wing; $\emptyset$, approximately 11.6°.)

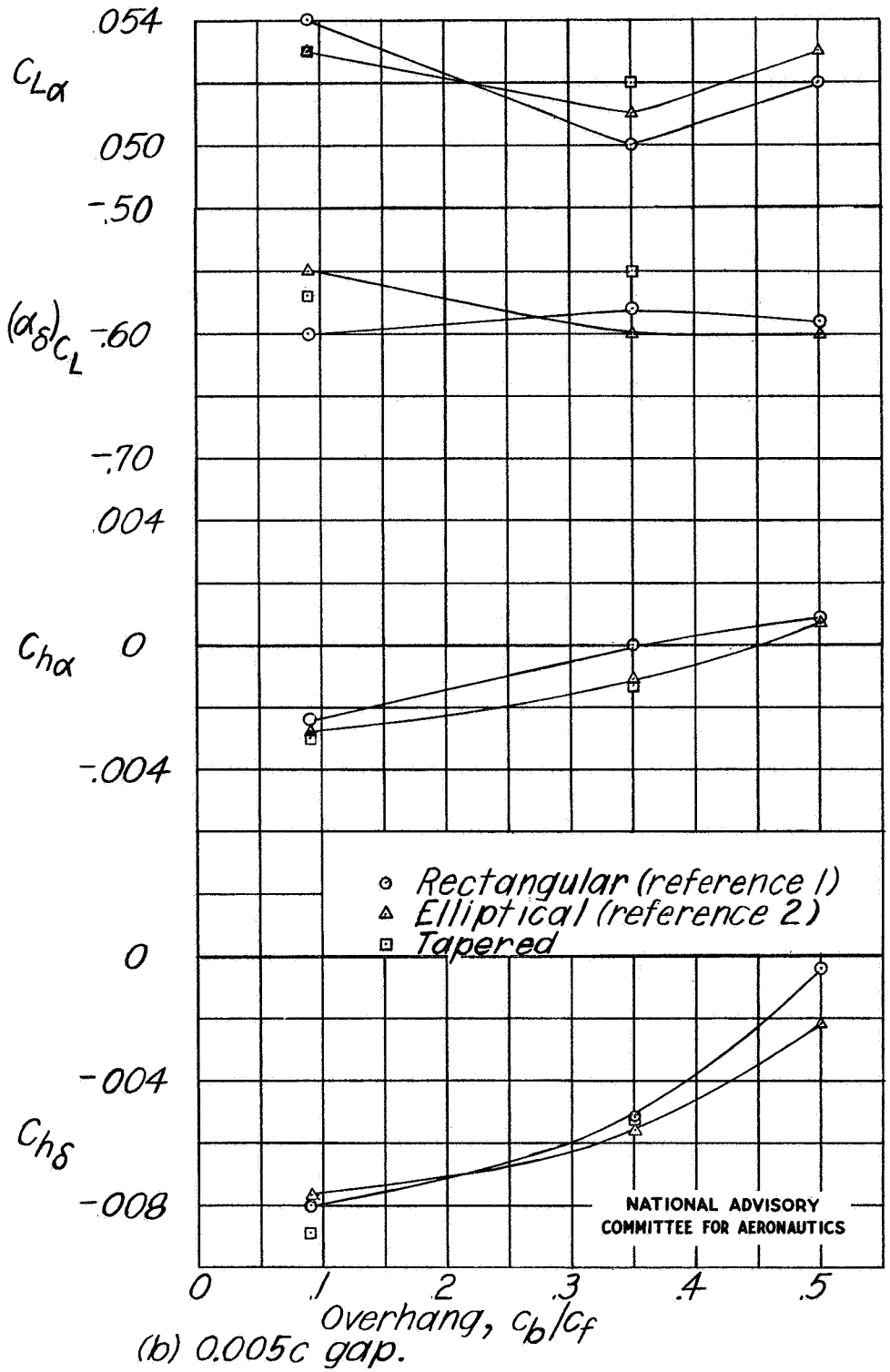

(b) 0.005c gap.

Figure 15.-Concluded.

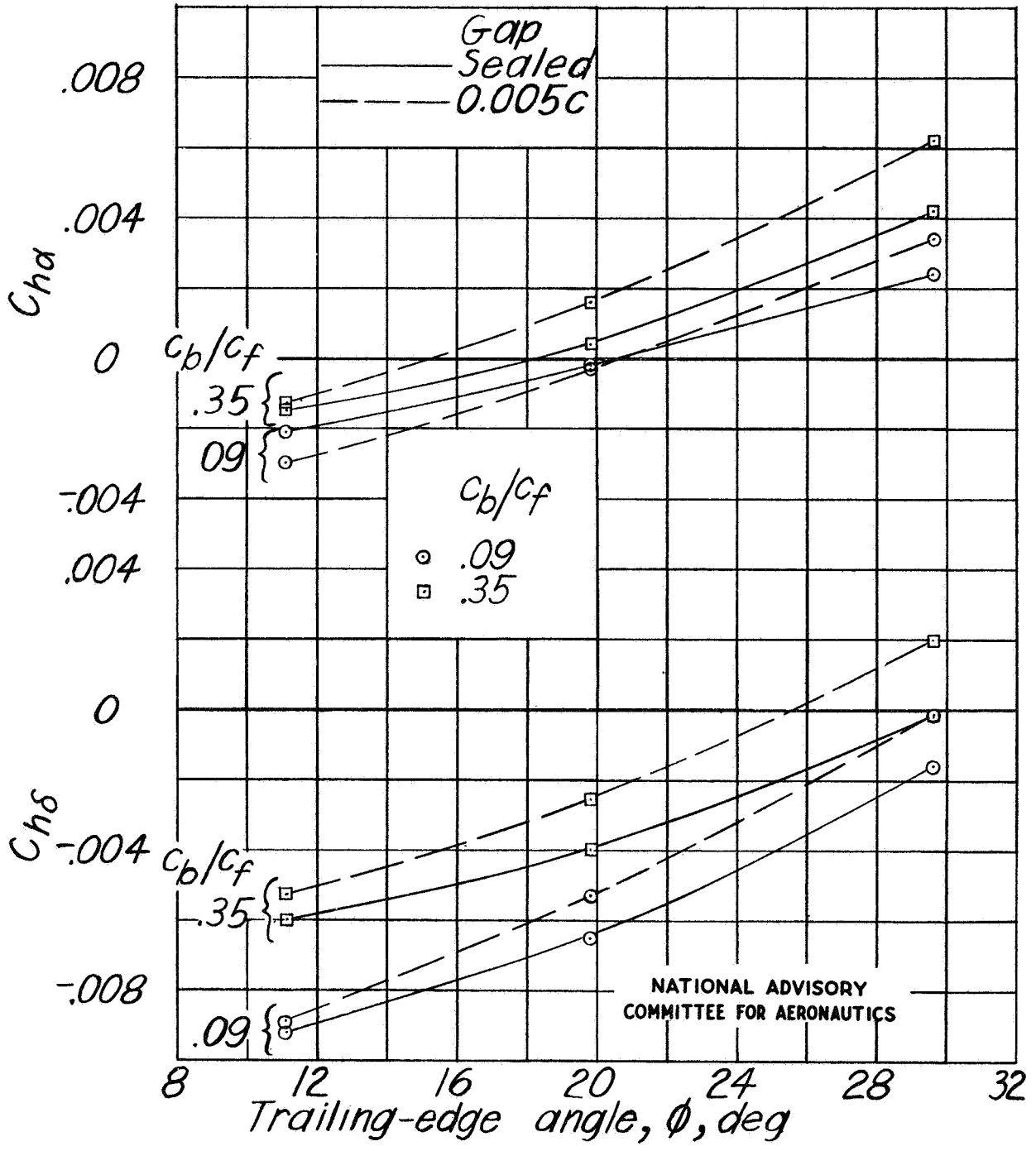

Figure 16.-Variation of flap hinge-moment parameters with trailing-edge angle for a tapered semispan wing. 0.30c flap; A=3.

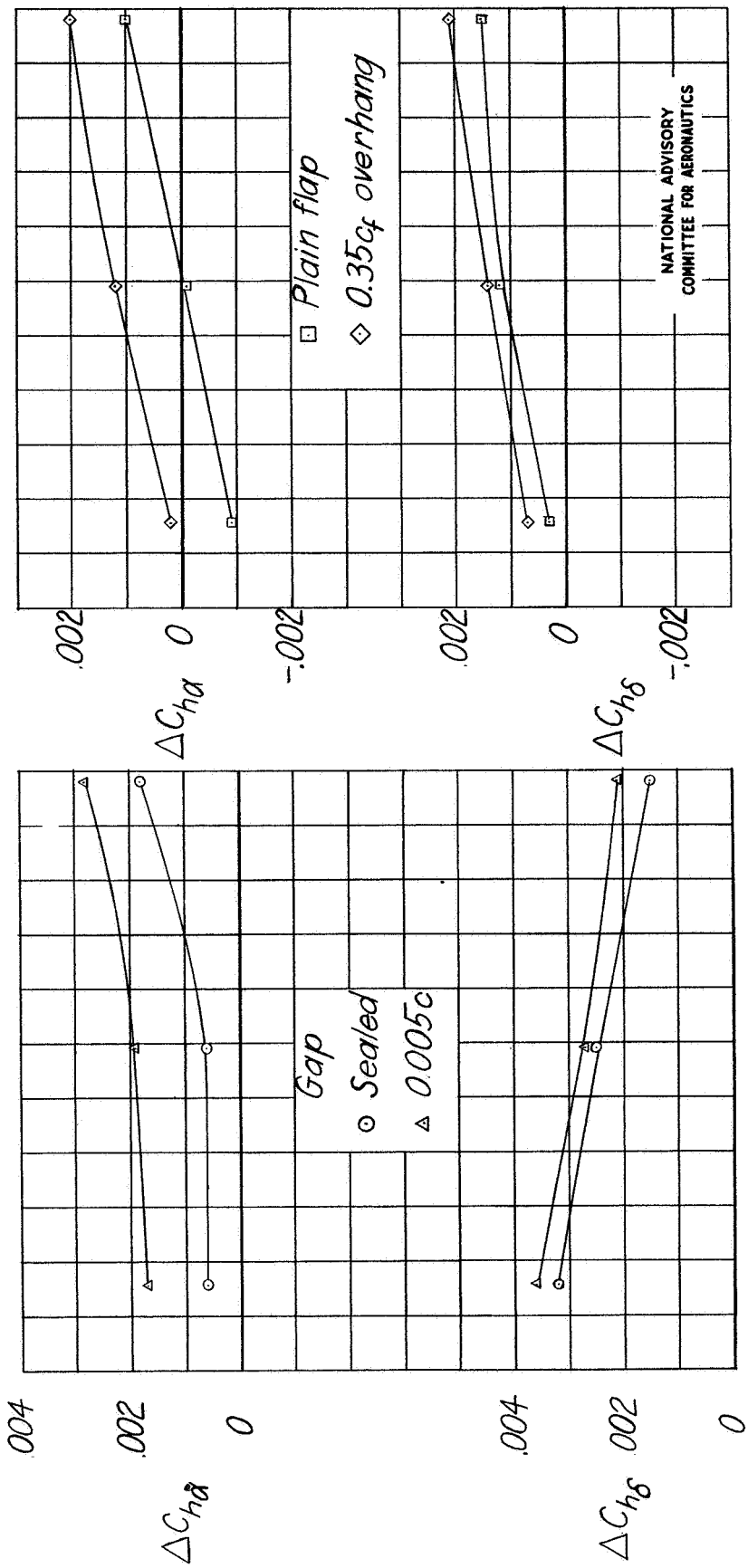

(a) Produced by 0.35c_f overhang.

(b) Produced by gap condition.

Figure 17.-Effect of trailing-edge angle on the increments of the hinge-moment parameters produced by increasing the overhang or by unsealing the gap.

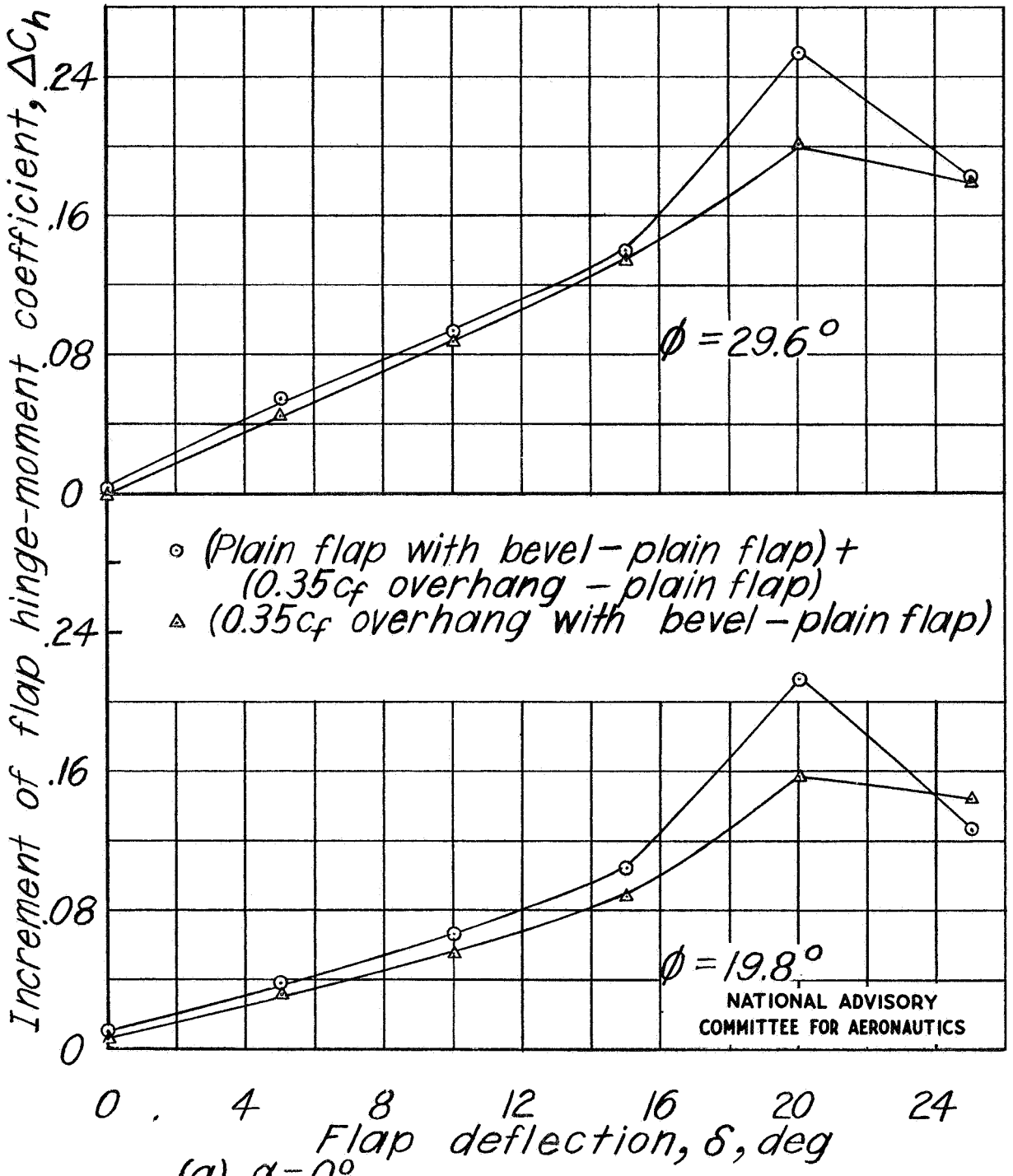

(a) $\alpha = 0°$.

Figure 18.-Comparison of effect on flap hinge-moment coefficient of bevel and overhang when found separately and in combination on a tapered semispan wing with a 0.30c sealed flap. A = 3.

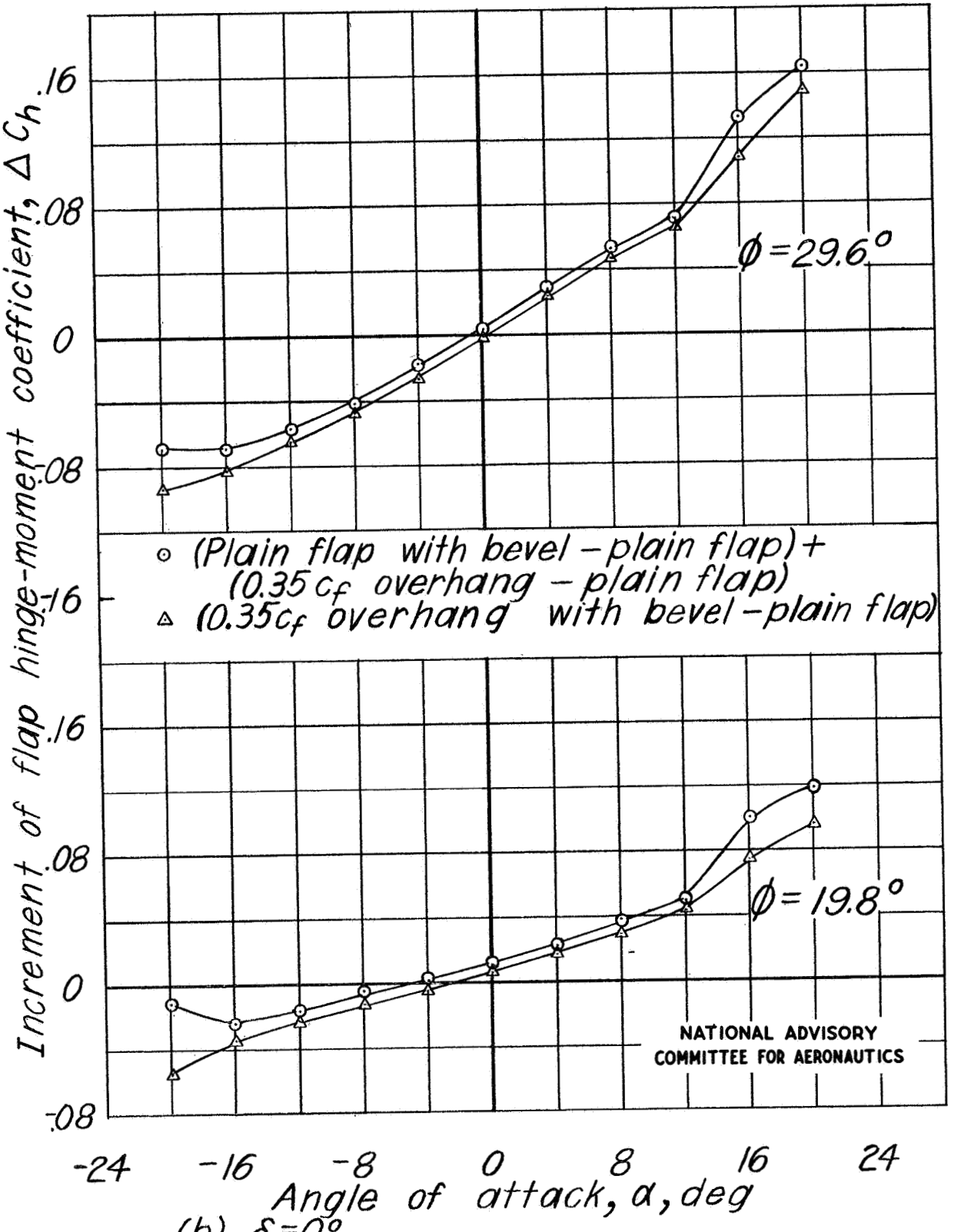

(b) $\delta = 0°$.

Figure 18.- Concluded.

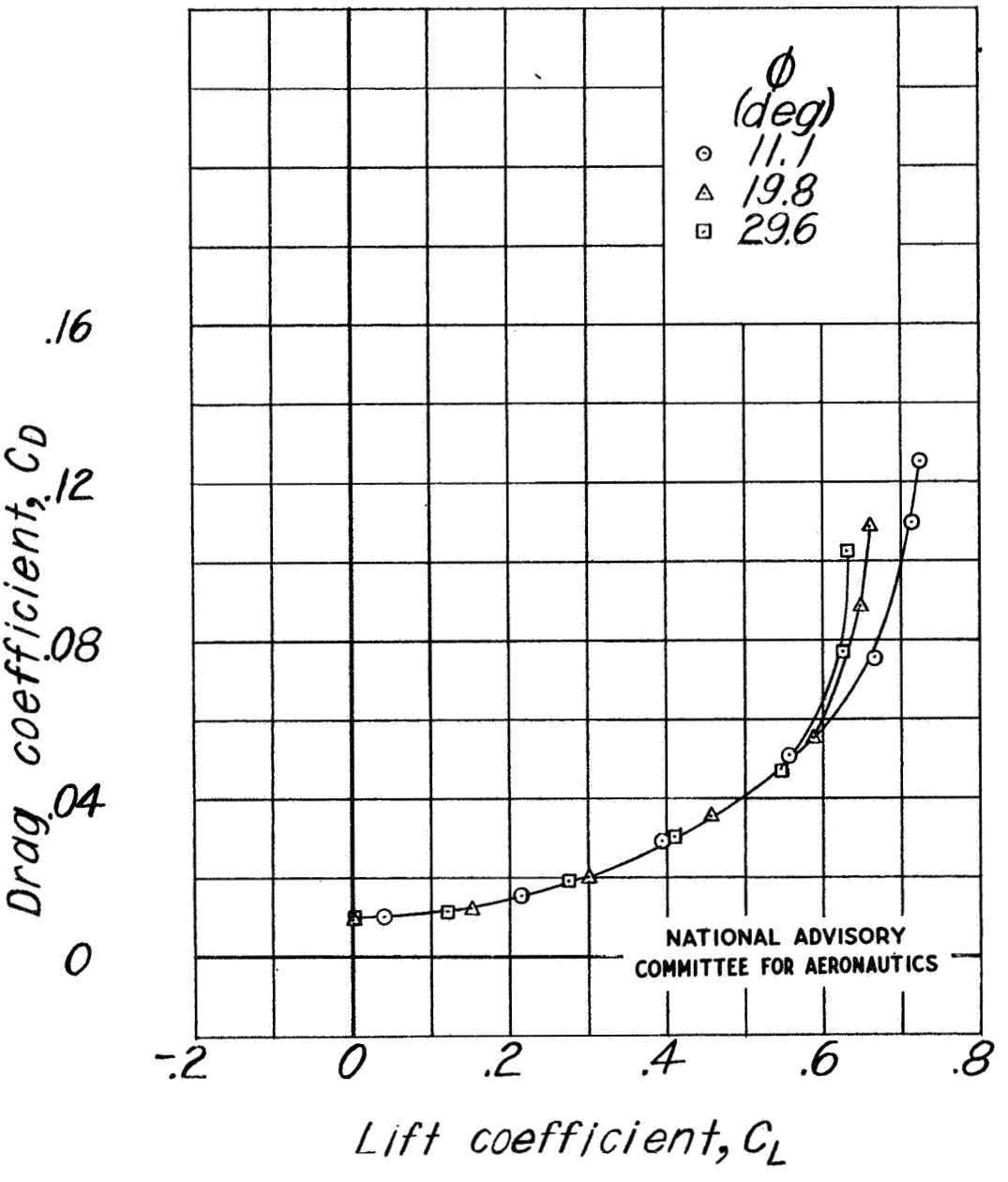

Figure 19.- Drag coefficient as a function of lift coefficient for a tapered semi-span wing with a 0.30c plain sealed flap having various trailing-edge angles. $\alpha = 0°$; $A = 3$.

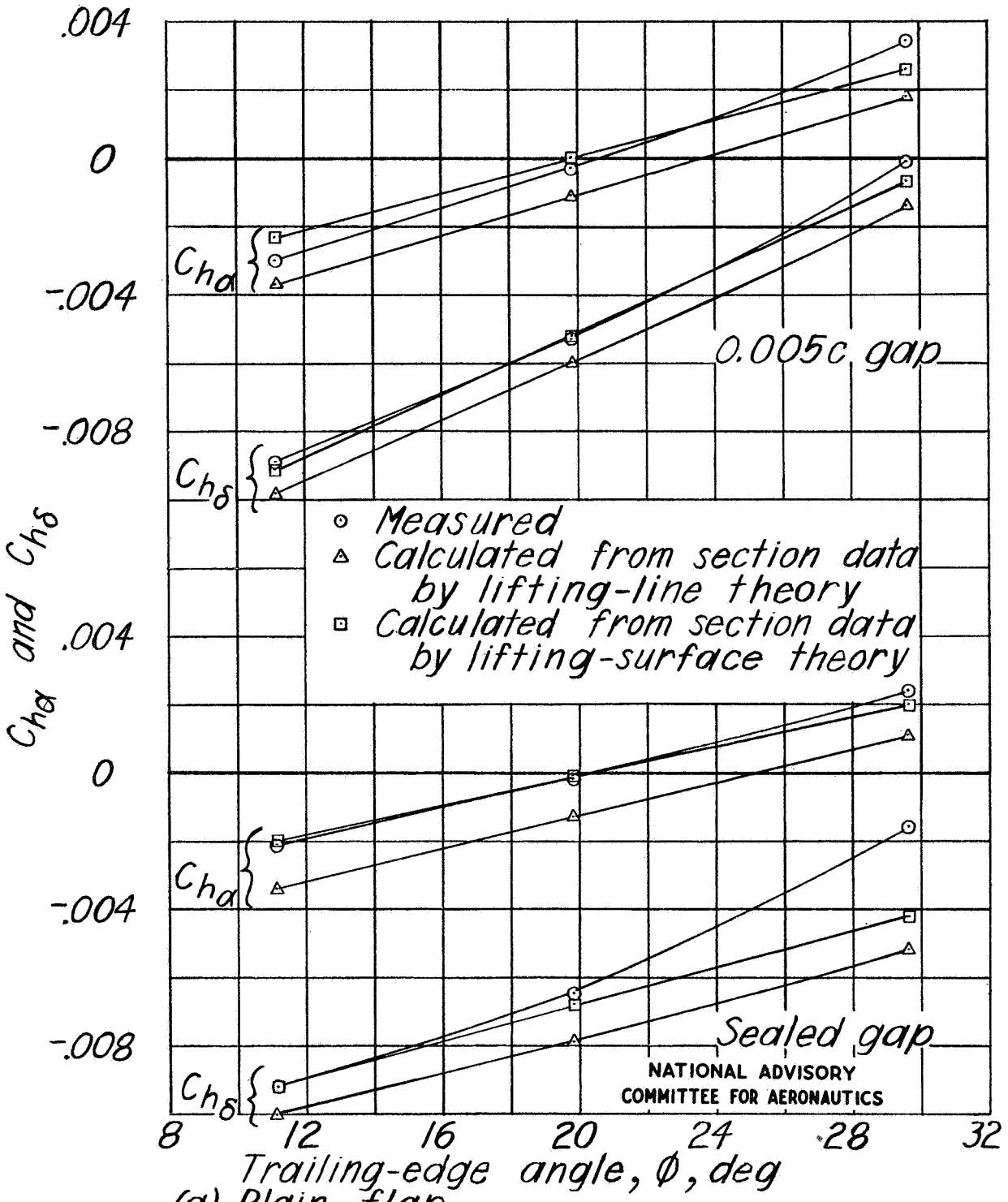

(a) Plain flap.

Figure 20.- Variation of flap hinge-moment parameters with trailing-edge angle for a tapered semispan wing. 0.30c flap; A=3.

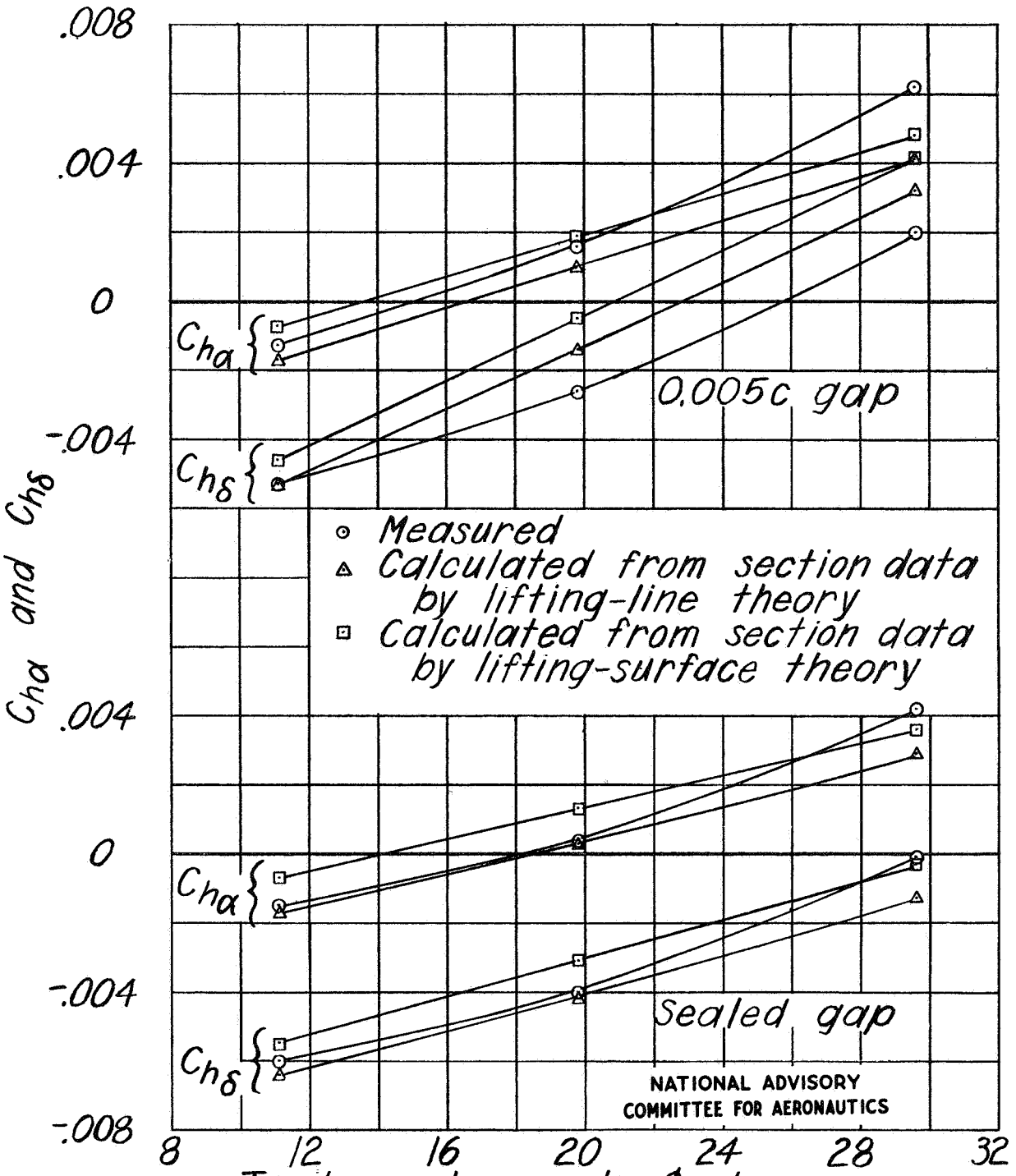

(b) $0.35c_f$ overhang.

Figure 20.-Concluded.